atmosphere

MDPI

Review

Tropical Atlantic Variability: Observations and Modeling

William Cabos [1,2,*], Alba de la Vara [3,4] and Shunya Koseki [5]

1 Department of Physics, University of Alcalá, 28805 Alcalá de Henares, Spain
2 Alfred Wegener Institute for Polar and Marine Research, 27570 Bremerhaven, Germany
3 Environmental Sciences Institute, University of Castilla-La Mancha, Avenida Carlos III s/n, 45071 Toledo, Spain
4 Departamento de Matemática Aplicada a la Ingeniería Industrial, E.T.S.I. Industriales, Universidad Politécnica de Madrid, c/José Gutiérrez Abascal, 2, 28006 Madrid, Spain
5 Geophysical Institute, University of Bergen and Bjerknes Centre for Climate Research, 5020 Bergen, Norway
* Correspondence: william.cabos@uah.es

Received: 20 July 2019; Accepted: 19 August 2019; Published: 27 August 2019

Abstract: We review the state-of-the-art knowledge of Tropical Atlantic Variability (TAV). A well-developed observing system and sustained effort of the climate modeling community have improved our understanding of TAV. It is dominated by the seasonal cycle, for which some mechanisms have been identified. The interannual TAV presents a marked seasonality with three dominant modes: (i) the Atlantic Zonal Mode (AZM), (ii) the Atlantic Meridional Mode (AMM) and (iii) the variability in the Angola–Benguela Front (ABF). At longer time scales, the AMM is active and low-frequency variations in the strength, periodicity, and spatial structure of the AZM are observed. Also, changes in the mean position of the ABF occur. Climate models still show systematic biases in the simulated TAV. Their causes are model-dependent and relate to drawbacks in the physics of the models and to insufficient resolution of their atmospheric and oceanic components. The identified causes for the biases can have local or remote origin, involving the global ocean and atmospheric circulation. Although there is not a clear consensus regarding the role of model resolution in the representation of the TAV, eddy-resolving ocean models combined with atmospheric models with enhanced horizontal and vertical resolutions simulate smaller biases.

Keywords: Tropical Atlantic Variability; Tropical Atlantic climate; sea-surface temperature biases; observational data; climate modeling

1. Introduction

The climate in the Tropical Atlantic (TA) shows significant seasonal to decadal (and longer) variability (see e.g., [1–7]). This is characterized by strong sea-surface temperature (SST) variability in the equatorial Atlantic Cold Tongue (ACT), where the amplitude of the SST seasonal cycle can reach 5–7 K [8]. Also, in the southeastern tropical Atlantic (SETA), strong seasonal and interannual variability is observed in the coastal upwelling regions near the Angola–Benguela front (ABF, see Figure 1; e.g., [9,10]). The variability of the climate system in the TA shows an inherently atmosphere–ocean coupled behavior in which the evolution of the oceanic currents and upwelling systems is closely linked to the evolution of the West African Monsoon, as well as to oceanic/land pressure systems. Changes in the large-scale atmospheric systems lead to an associated meridional displacement of the Intertropical Convergence Zone (ITCZ) and variations in regional surface winds [11]. In turn, these atmospheric changes drive large- and regional-scale variations in the dynamics of the Tropical Atlantic Ocean. This variability is modulated by several factors such as the regional air–sea interactions [12–14], the complex

geometry of the Atlantic basin [15] and external factors—mainly the North Atlantic Oscillation (NAO) and the El Niño Southern Oscillation (ENSO; [16–18]). See also [1,4] and references therein.

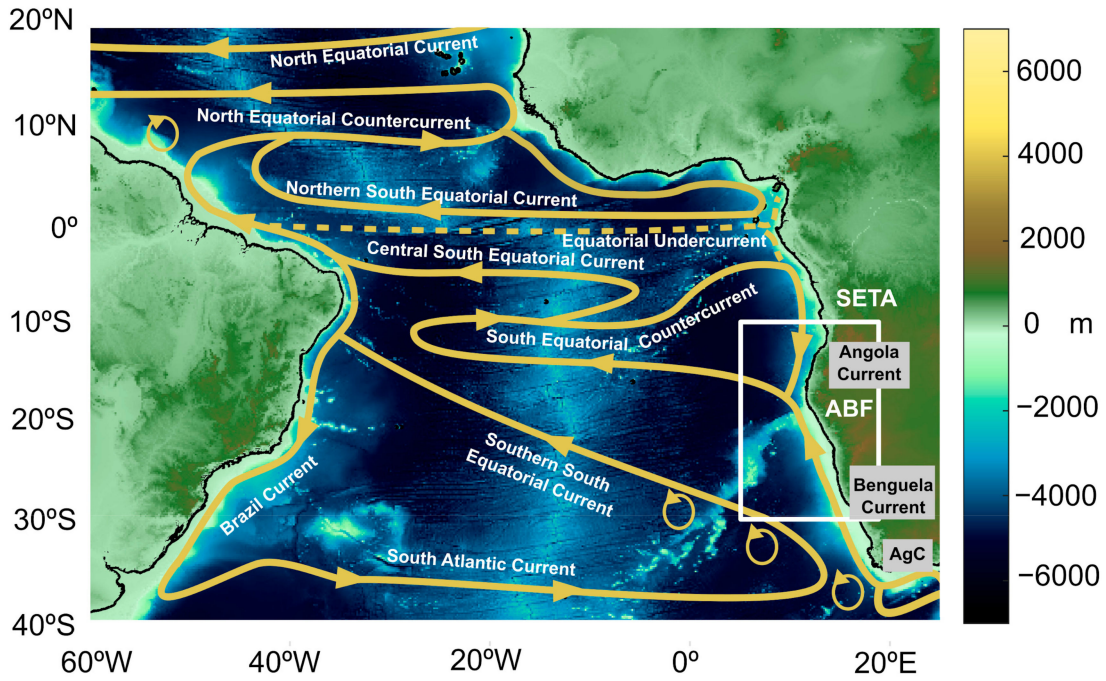

Figure 1. Bathymetry of the Tropical Atlantic in which the configurations of the main near-surface currents are depicted. AgC refers to the Agulhas Current. In this figure, the Southeastern Tropical Atlantic (SETA) and Angola–Benguela Front (ABF) regions are also highlighted.

The Tropical Atlantic climate is sensitive to changes in global oceanic circulation and the global hydrological cycle, as the Tropical Atlantic is connected to the southern and northern branches of the Atlantic Meridional Overturning Circulation and receives freshwater inputs from some of the world's largest rivers. All these factors set the characteristics of the Tropical Atlantic variability (TAV) at seasonal, interannual, and even longer timescales. Starting from the interannual variability, this can be represented by its two leading SST modes. The most relevant one is the Atlantic Zonal Mode (AZM; [4,19,20]), which is governed by the equatorial ocean dynamics in response to surface winds, like ENSO in the Pacific. This mode involves changes in the equatorial Atlantic cold tongue and results in a concomitant vertical displacement of the equatorial thermocline. The second one, referred to as the Atlantic Meridional Mode (AMM), is characterized by a cross-equatorial gradient of SST and wind anomalies [17,21]. Their patterns and seasonality will be addressed in detail later in the text.

The variability in the TA largely influences the climate of the surrounding areas, weather, and marine ecosystems, among others. Thus, its accurate prediction at seasonal and decadal timescales and consistent projections by climate models are highly demanded by society, industry, and stakeholders in order to prevent and mitigate potential damages associated with the tropical Atlantic SST variability (e.g., [5,22–32]). Notwithstanding the rapid development of computational resources and improvements in the representation of physical processes and numerical formulation, state-of-the-art climate models are still not able to make accurate climate predictions. Therefore, climate projections under global warming scenarios are uncertain in the region. This shortcoming may be closely related to problems of climate models to reproduce the TA SST. In this respect, most models exhibit large and systematic SST biases in the TA (e.g., [33–36]). To make this picture more complex, detected sources of the biases are largely dependent on the particular climate model used.

The aim of this paper is to provide a general insight of the state-of-the-art of our knowledge of the Tropical Atlantic Variability. We do not address in detail the different aspects related to the TAV to keep the paper concise. Besides, recently, some good reviews about the observing system in the Tropical

Atlantic (e.g., [5,6]), the Atlantic modes of variability [4] or modelling the TA climate (e.g., [7]) have been published. Instead, we try to give an overview of these topics in a concise manner, and the reader can resort to the specific reviews mentioned above for detailed information regarding one of these specific topics. This paper is structured as follows. In Section 2, we briefly review the observational system that provides data used for observational studies, model verification, and data assimilation in operational and reanalysis systems. In Sections 3 and 4, we present the current state of our understanding of the seasonal and interannual aspects of the Tropical Atlantic variability. In Section 5, we provide a brief review of questions related to the low-frequency variability in the region. We discuss how realistically the state-of-the-art coupled models reproduce the variability in Section 6. Finally, in Section 7, the conclusions and outlook are given.

2. Observational Data

Here, we present the state-of-the-art in the observational aspects of the TAV. In this section, we follow [5], where an extensive review of the observing system in the Tropical Atlantic is given with a more detailed enumeration of the implied observational infrastructure.

2.1. Observing System

A better understanding of the TAV and the improvement of its representation in climate models demands a well-developed observing system. The elements of this observing system can be quite different in deployed capacity, technical implementation, spatial coverage, and the amount of data they provide. Moreover, their coverage varies within different regions and is composed by in situ observations (mooring arrays, Repeat Hydrographic Surveys and Ships of Opportunity, Surface drifting buoys) and satellite observations.

A great amount of in situ measurements derive from the Prediction and Research Moored Array in the Tropical Atlantic (PIRATA) project (see Figure 2 of [5,6]), which currently consists of 18 moorings that measure ocean temperature and salinity in the upper oceanic layers, near-surface air temperature, relative humidity, wind velocity, rainfall, and incident shortwave radiation. Several moorings also measure downward longwave radiation, atmospheric pressure, and surface ocean currents. PIRATA provides daily-averaged data in real-time but the frequency of data transmission is being upgraded to hourly averages. PIRATA is complemented by other smaller and more recent mooring systems. Another important source of in situ measurements are the Argo array of autonomous floats. They make profiles of temperature, salinity, and pressure in the upper 2000 m typically every 10 days [37]. Argo is expanding its measurement capabilities to include full-depth (4000–6000 m) profiles [38], with nine deep floats in the TA (see Figure 2B of [5]). These Argo deep floats will constitute a good addition to the Global Ocean Ship-based Hydrographic Investigations Program (GO-SHIP), which carries out high-quality, full-depth measurements in the global ocean approximately once every ten years. The measurements from the GO-SHIP have high horizontal and vertical resolutions and measure many different physical, chemical, and biological variables along several sections near the western and eastern boundaries of the TA (see Figure 10 of [5]).

Operational data also comes from cruises. In this context, it is important to highlight the important contribution of the ship-of-opportunity program (SOOP) and PIRATA. On one hand, the volunteer merchant ships that participate in SOOP regularly traverse three transects in the TA, each of them repeated approximately every 3 months (see Figure 10 of [5]). They measure the sea-surface salinity (SSS), SST, and temperature in the upper 760 m. With the collected data, ocean large-scale circulation and mesoscale variability can be deduced. On the other hand, the annual PIRATA servicing cruises provide opportunities for repeated shipboard measurements and deployments of Argo floats, surface drifters, ozone sondes, radiosondes and for water sample analysis to determine the concentrations of the different dissolved components of the sea water.

A special mention deserves the array moorings and pressure-equipped inverted echo sounders that have been installed to measure the shallow boundary currents and the deep western boundary

currents at the Brazilian continental slope [39,40], the Angola Current [41], and the deep flow between the continental slope and the mid-Atlantic ridge (see Figure 1; [42,43]). These arrays contribute to the AMOC observing system. Figure 10 of [5] shows the locations of the boundary current arrays and inverted echo sounders.

Surface drifters follow the ocean surface current, measuring the ocean surface circulation at high resolution, and relaying the data via satellite. They measure SST, surface currents, and barometric pressure and a few of them also collect subsurface temperature, surface and subsurface salinity, wind velocity, and directional wave spectra. As part of the Global Drifter Program (GDP), an average of 92 drifters provide measurements at approximately hourly frequency (Figure 2 of [5]).

Satellites provide large amounts of data in real-time or near real-time regarding the ocean and the atmosphere. For instance, they allow us to obtain estimates of SST, tropical rainfall, precipitable water, sea-surface height (SSH), and, beginning from 2009, SSS at high spatial resolution (0.25°). Available satellites achieve a complete coverage of the TA in a few days. Satellite observations allow us to improve the estimation of heat, moisture, and momentum surface flux estimates with better coverage, resolution, and accuracy [44].

2.2. Reanalysis

In a reanalysis, observations are assimilated by a numerical model that generates a synthesized estimate of the state the ocean and/or the atmosphere. They provide climatic information about the ocean and the atmosphere that covers the entire globe. State-of-the-art reanalysis systems reconstruct the recent past climate of the Earth and include the atmosphere, the ocean, the land, and waves and sea ice (an up-to-date list of available reanalyses is keep in https://reanalyses.org/). The last generation of ocean-atmosphere coupled reanalyses, as the Climate Forecast System Reanalysis (CFSR) [45] and the Coupled ECMWF *ReAnalysis* of the Twentieth Century (CERA-20C) [46], take into account air–sea interactions. These reanalyses therefore provide a more physically consistent state of the two components of the climate system. CFSR has an atmospheric resolution of ~38 km and an oceanic resolution of ~0.25° at the equator. The horizontal resolution of CERA-20C is ~25 km in the atmosphere and ~37 km in the ocean at the equator. Due to their global coverage and availability of data over long timescales, reanalyses can be used for the identification of the mechanisms of climate variability. A major advantage of reanalysis is that they provide all atmospheric and/or oceanic variables without spatial or temporal gaps. Also, the values of the different variables are constrained by the data assimilation, which avoids large differences between data and observations. Although assimilation helps to maintain the climate simulated by the numerical model used in the reanalysis close to the observations, it also brings unphysical forcings and some caution should be taken when using reanalysis data.

3. Seasonal Variability of the TA Climate

TAV involves changes on the seasonal time scale and is largely affected by the adjacent continents. For instance, in the eastern equatorial Atlantic, surface winds, convective activity, and SST feature a marked seasonal cycle ([47]; see Figure 2 for the seasonal cycle of SST). Changes in the SST in the equatorial Atlantic do not have an equal duration: the seasonal cycle of the SST in the equator is characterized by a rapid cooling, which peaks after three months, while it takes about nine months to warm up the region. The cooling lasts from April to July and is caused by strong southeasterly winds close to the equator. These winds produce upwelling (downwelling) and elevate (deepen) the thermocline to the south (north) of the equator. The cooling intensifies the contrast between warmer waters north of the equator and colder waters south and at the equator [48]. The low SST along the equator in the Gulf of Guinea gives place to the ACT, which lasts the whole austral winter (June-July-August; JJA). In turn, interannual SST variations within the ACT region profoundly affect precipitation over West Africa and modulates the onset of the West African monsoon [30,49,50]. The presence of the ACT creates a strong temperature gradient between ocean and land that is associated

with a further strengthening of southerly winds. The seasonal ACT and the intensified winds coincide with the northward migration of the rainband away from the equator onto the West African continent, with intense precipitation reaching as far north as 15° N in boreal summer. The SST in this region attains the maximum values in austral spring, when the ITCZ is closest to the equator.

In this context, [15] proposed that the annual cycle in the eastern equatorial Atlantic is set by continental monsoons, while local air–sea interactions only have a secondary influence. In contrast with this, [51] suggested that ocean–atmosphere interactions play an important role in the march of the seasonal cycle in the region. They hypothesized that the ACT intensifies the southerly winds in the Gulf of Guinea and these push the rainband further north over the land. Supporting this point of view, more recent studies have found that meridional SST and sea-level pressure (SLP) gradients are closely related to meridional winds over the Gulf of Guinea [52–54]. While it is widely accepted that the impact of the continental West African summer Monsoon (WAM) on ocean surface winds contributes to a lowering of the SST, the importance of the SST cooling for the development of the monsoonal winds, and subsequently the precipitation, is still debated. For instance, ref. [55] suggested that the generation of the ACT is not very important for the development of the WAM, although this has an impact on its strength.

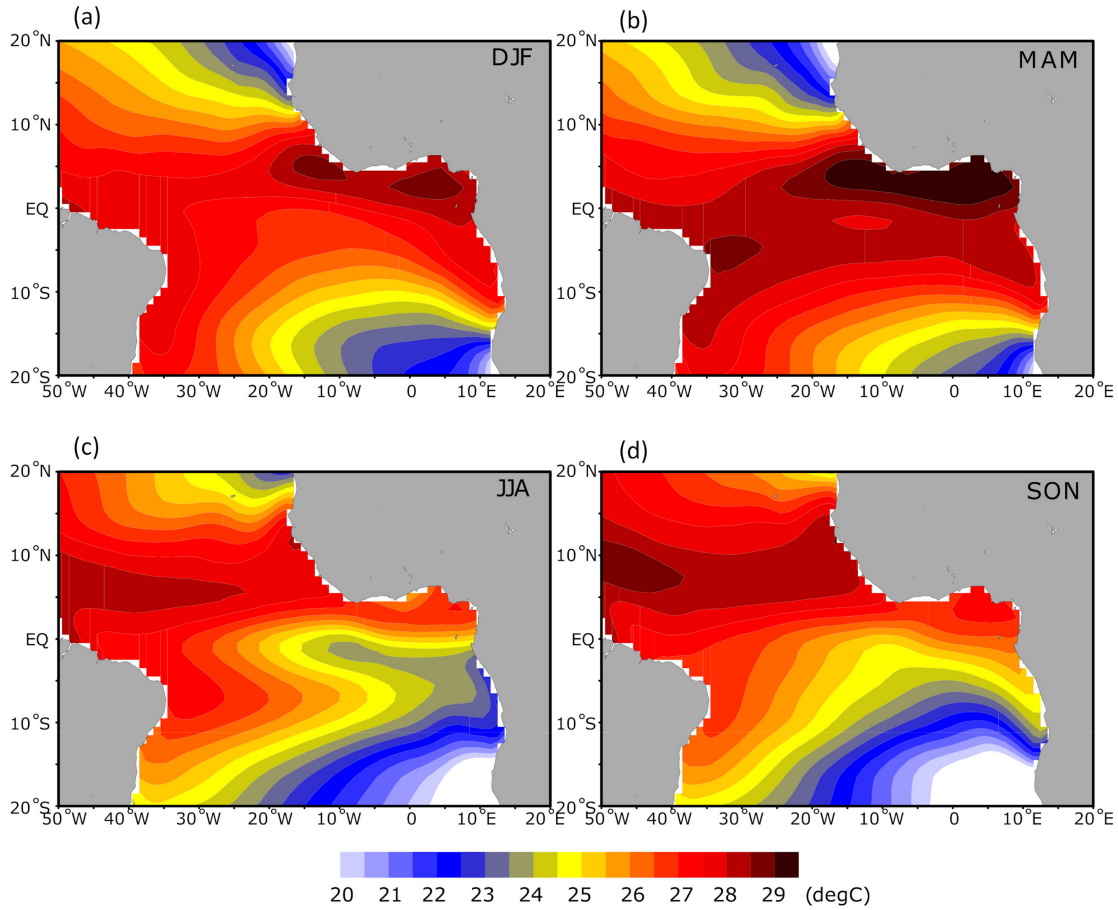

Figure 2. *Cont.*

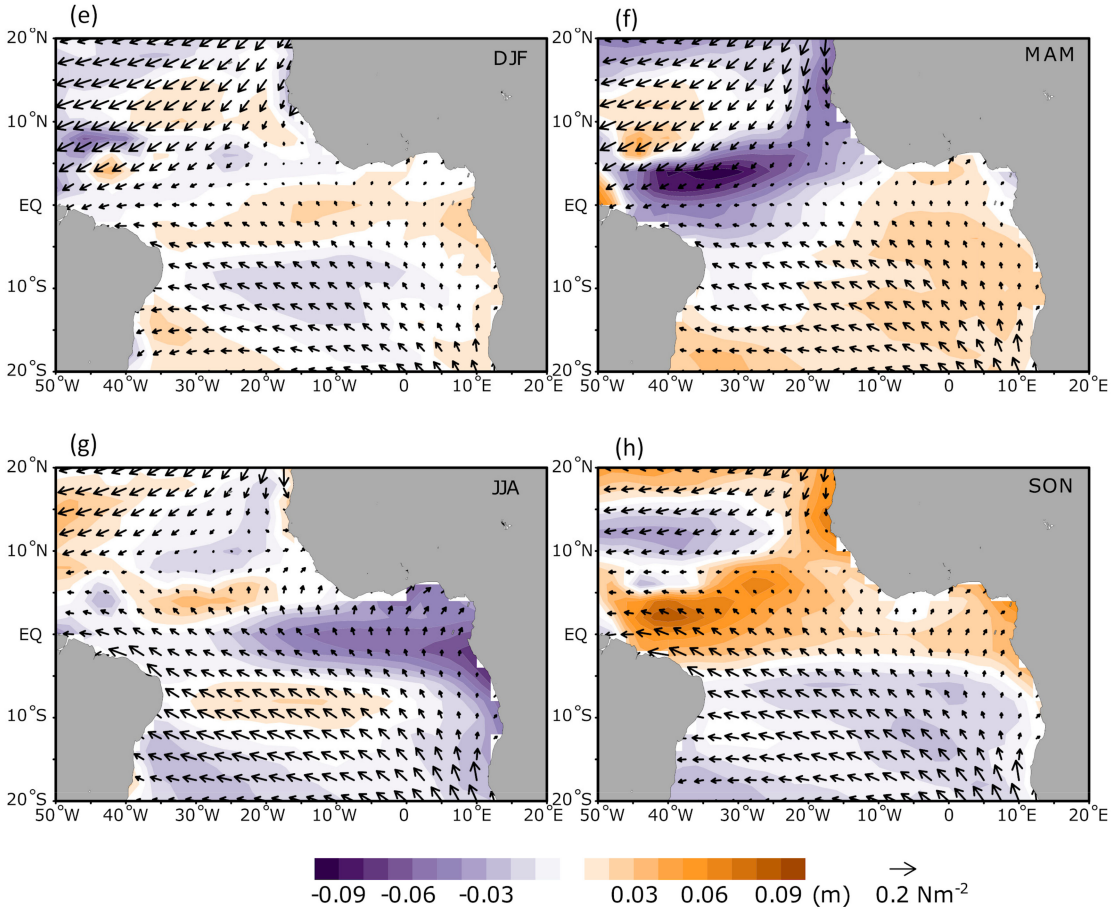

Figure 2. (**a**–**d**) Climatology of seasonal sea surface temperature obtained from TropFlux (1979–2011) (https://incois.gov.in/tropflux/index.jsp; accessed on 12 June 2019). (**e**–**h**) Climatology of surface wind stress obtained from ERA-Interim (1979–2011) and seasonal anomaly of sea surface height from annual-mean obtained from AVISO (1993–2000). December-January-February (DJF); March-April-May (MAM); June-July-August (JJA); September-October-November (SON).

Regarding the western equatorial Atlantic, there is a consensus that in this region, ocean–atmosphere interactions are important for the seasonal cycle of the ITCZ, surface winds and the SST. In particular, a strong dependence of the seasonal cycle of surface winds in this region on the underlying SST was identified. It was also found that surface wind convergence in this region is rather related to convective heating anomalies than to the underlying SST and SLP gradients [53]. Recently, using a global atmospheric model, the authors of [54] tried to shed light on this controversy. They found, in greater agreement with [51], that seasonal variations of precipitation over the equatorial Atlantic are influenced by both the land and the ocean, with land surface temperatures being the main driver of the continental rainfall. In accord with all previous results, they concluded that the coupling between the ocean and the atmosphere plays a more important role in the western than in the eastern equatorial Atlantic. Regarding the mechanisms of the seasonal variability, they found that the seasonal evolution of the equatorial SST and the winds in the western equatorial Atlantic is consistent with the positive Bjerknes feedback (see also [34]). They also concluded that a mechanism similar to the wind-evaporation–SST feedback [56] might play a role in the western equatorial Atlantic. Finally, they proposed that the pressure adjustment mechanism [57] could explain most of the variability in the eastern Atlantic, but not in the central equatorial Atlantic, which can be influenced by the extratropical interhemispheric differential heating that controls the large-scale Hadley Circulation.

Along with this, the South Atlantic Anticyclone (SAA) also experiences seasonal changes in its position and intensity. This structure forms due to convective processes within South Africa

and South America in combination with orographic effect with midlatitude westerly winds and trade easterlies [58,59]. In addition to this, the SAA is also set by cross-hemispheric effects of heat sources located in the Northern Hemisphere [60]. The combination of these mechanisms results in an intensification of the SAA in austral winter relative to austral summer. In austral summer, the strength of the SAA has been linked to ocean–atmosphere interactions [61]. In more detail, in [61] it is claimed that, in austral summer, the strengthening of the SAA relates to an enhanced SST zonal gradient. This is sustained by warming in the western flank of the TA and cooling to the east of this basin. On the one hand, southward heat transport from the equator to the south by the Brazilian current favors advection of warmer air in the lower troposphere. On the other hand, colder conditions are maintained to the east due to the development of the coastal Benguela upwelling system, which brings colder waters to the surface. In contrast with this, it has also been proposed that the zonal gradients of SST only play a minor role in the seasonal cycle of the SAA [33]. However, [34] suggested that conclusions from [33] could be affected by the use of an uncoupled model and the fact that they only focus on the winter season, when SAA is set by the monsoon [62]. Another mechanism related to the zonal SST anomalies in the TA has been proposed by [59]. They suggest that cold and warm anomalies act as sources of anticyclonic and cyclonic potential vorticity and induce along-shore wind anomalies towards the equatorial Atlantic.

4. Interannual Variability in the TA

4.1. Climatological Patterns

The interannual TAV also presents a marked seasonality. Figure 3 shows the seasonal cycle of the SST variability in the TA deduced from observations and reanalysis data. At the equator, the interannual variability peaks in summer (June to July) in the central equatorial Atlantic (20° W–0°) in Figure 3a. The large variability extends to the western African coast. Another weaker peak appears in winter (November to January) with less extending range. As previous studies concluded, the equatorial variability is firmly phase-locked to summer (e.g., [63–66]), while the variability in the tropical Pacific has a peak in winter (November to January) (e.g., [67]). The horizontal distribution of the summer TAV is given in Figure 3b. In general, the equatorial TAV distributes in a L-shaped form from the Gulf of Guinea to the ABF region and influences the precipitation activity along the western African region (e.g., [68]). This L-shaped variability shows us that the equatorial variability is closely related to the variability in the ABF region (e.g., [64,69]; [4] and references therein).

Figure 3c presents the climatological seasonal cycle of the SST variability in the ABF region. In contrast to the equatorial variability (Figure 3a), the SST variability is maximized in spring (March to April) along the southwestern African coast. In spring, the SST variability is limited in the coastal region and the equatorial variability is quite modest (Figure 3d), indicating that the SST variability in the ABF leads the equatorial SST variability in summer by about three months (e.g., [64]). Variability is also high to the northeast Atlantic coast (Figure 3b,d). This region is associated with the Senegal–Mauritania upwelling system and recently it has been found that this interannual variability is detected as Dakar Niño/Niña [70]. However, the connection between the equatorial and northeastern Atlantic variability has not been discussed yet.

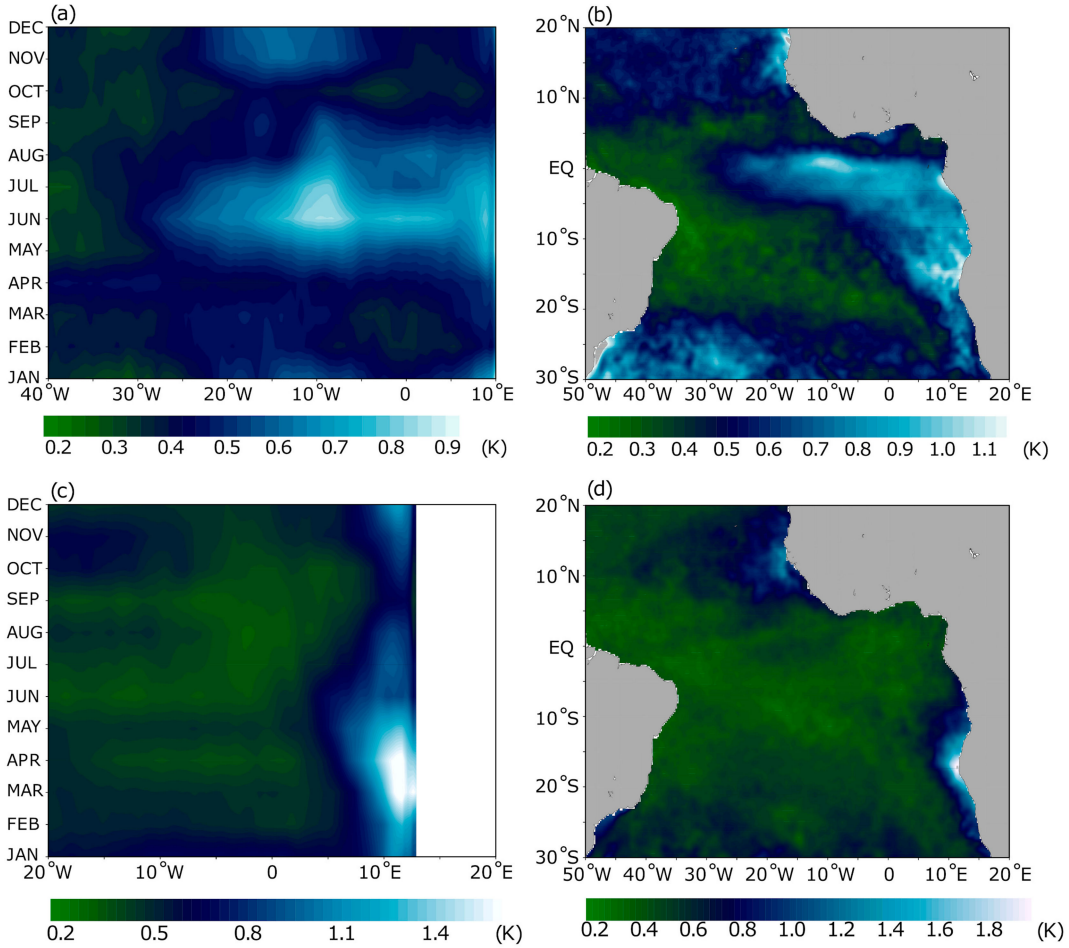

Figure 3. (**a**) and (**c**) seasonal cycle of the observed sea-surface temperature (SST) (OISST, 1979–2010) one standard deviation in the Equatorial (averaged between 3° S and 3° N) and Angola–Benguela Frontal Zone (averaged 20° S–14° S). The observed SST standard deviation in (**b**) June and (**d**) March, respectively.

4.2. Atlantic Zonal Mode

The interannual TAV consists of some leading climatic modes. Perhaps the most relevant one is the so-called Atlantic Zonal Mode (AZM; e.g., [71]), often referred to as Atlantic Niño mode. AZM is detected as a first mode of the Empirical Orthogonal Function (EOF). Figure 4a shows the horizontal distribution of the first EOF mode of monthly SST anomalies from observations. The EOF mode is calculated by 12-month anomalies from each monthly climatology. The first EOF mode features an L-shaped which extends from the southwestern African coast toward South America in the equatorial Atlantic. This distribution is quite similar to that of standard deviation of the SST in June (Figure 3b). This first mode is observed frequently in June, as shown in Figure 4b of principal component (PC) score of this mode and the mode varies from warm to cold phases in several years temporal scale. In particular, the warm (cold) phases of this mode is regarded as Atlantic Niño (Niña) and has similar characteristics relative to the El Niño/La Niña variability in the tropical Pacific.

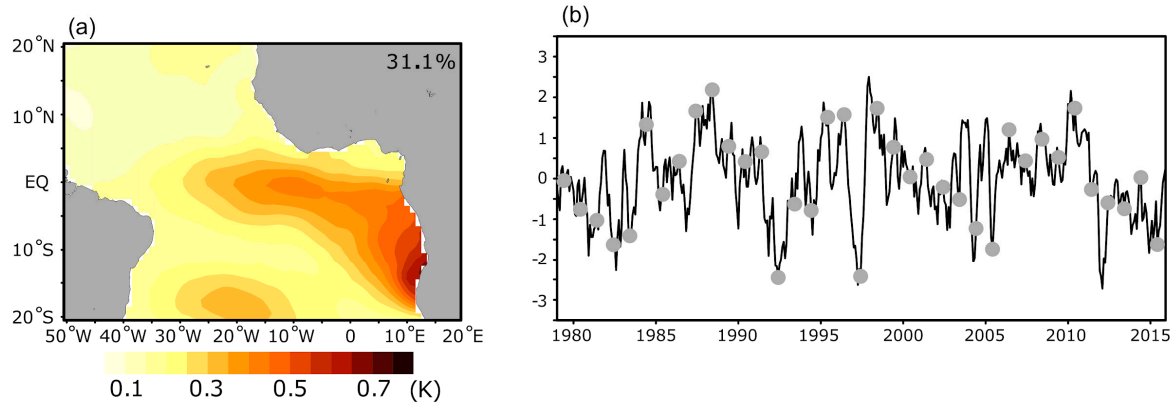

Figure 4. (**a**) Empirical Orthogonal Function (EOF) 1st mode for 12-monthly anomaly of SST (1979–2015) obtained from TropFlux and (**b**) its principal component (PC) score normalized by the standard deviation of the PC score. The gray dots denote the PC score in June for each year.

One of the most noticeable similarities between Atlantic and Pacific modes is related to their dynamics: the generation and maintenance of the AZM is considered to be demonstrated by the Bjerknes Feedback (BF) [72]. The first element of the BF is the connection between the equatorial SST and zonal surface winds variabilities, as shown in Figure 5a. The zonal surface winds respond sensitively to the equatorial central SST anomaly in the western basin of the equatorial Atlantic. This indicates that the warm SST anomaly in the equatorial Atlantic decelerates tropical trade winds in most of the equatorial Atlantic (acceleration by the cold SST anomaly, vice-versa). Conversely, the negative regression is found over the Gulf of Guinea. This component is important in the AZM since this connection describes the equatorial ocean–atmosphere interaction. For example, biased climate models cannot capture this interaction well and, consequently, fail to reproduce realistically the behavior of the TAV (e.g., [65,73,74]).

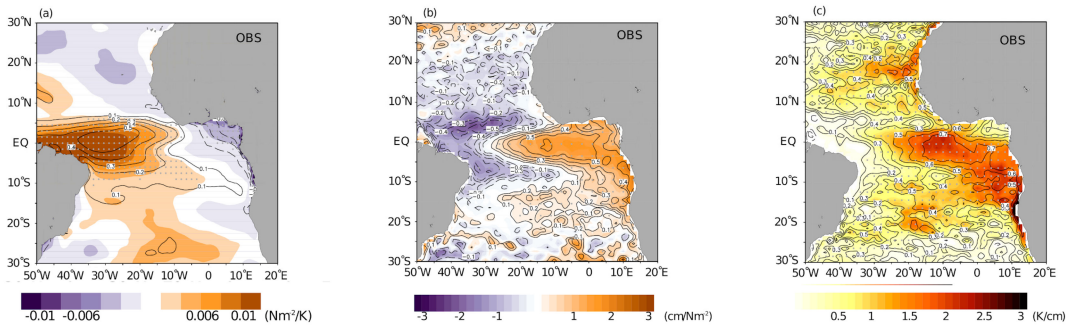

Figure 5. Three elements of Bjerknes Feedback (BF). (**a**) Correlation (contour, IC, 0.1) between ATL3 index (OISST) and zonal wind stress (ERA-Interim) and regression of zonal wind stress on ATL3 index. (**b**) Correlation (contour) between sea surface height (AVISO) and zonal wind stress (ERA-Interim) averaged over 2° S–2° N and 35° W–20° W and regression of sea surface height onto zonal wind stress averaged over 2° S–2° N and 35° W–20° W. (**c**) Correlation (contour) between grid-wise sea surface temperature (OISST) and sea surface height (AVISO) and regression (color) of sea surface temperature onto sea surface height. For the calculation, all 12-month anomalies (detrended) from monthly climatology are used. Similar figures are given by [63].

The second part of the BF is related to the internal ocean dynamics. Figure 5b shows the connection between the zonal wind stress over the western TA basin and the SSH anomalies (SSH is a proxy of thermocline depth). In the central to eastern equatorial Atlantic, SSH responds positively to the zonal wind stress. This pattern invokes us to the westerly anomaly of the zonal wind stress induces the downwelling in the sea surface to subsurface (deeper thermocline and higher SSH) and this signal travels eastward via equatorial Kelvin Waves. The upwelling in the Atlantic Cold Tongue region is

suppressed by the westerly anomaly over the western equatorial Atlantic. Moreover, the positive regression of SSH extends more southward along the West African coast until 15° S. As a result, the pattern of positive regression highly resembles that of the EOF first mode shown in Figure 4a. This can be extended through the coastal Kelvin Waves, which is considered to be a remote contributor to the interannual variability in the ABA (e.g., [69]). In contrast, the other upwelling in the Senegal–Mauritania region does not seem to be relevant for the equatorial Atlantic variability in this respect (there is very weak negative regression around 15° N)

The last piece of the BF is the association between the thermocline depth and the SST, shown in Figure 5c. This component describes that deeper thermocline depth (higher SSH) is attributed to the downwelling anomaly and, consequently, the SST becomes warmer due to less transport of cold water from the ocean subsurface. The highly positive regression is found in the equatorial Atlantic, Angola–Benguela area (ABA) and Senegal–Mauritania region, where the upwelling is vigorous and cold SST is associated with the upwelling (e.g., [75]). The downwelling anomaly in the ACT region induces the warm SST anomaly, and thus, the original SST warm anomaly in the first element of the BF is amplified by the downwelling anomaly propagating from the west.

The BF can be identified in the zonal mode of both the tropical Pacific and Atlantic interannual variability. However, the authors of [76] suggested some differences in the development of this mode and its feedback mechanism in the two basins. In the tropical Pacific, the zonal mode exhibits a clear asymmetry between warm and cold events with respect to strength, duration, and horizontal pattern (e.g., [76–78]). Accordingly, the intensity of each element of the BF also differs largely between the warm and cold events [76]. In contrast, the Atlantic mode shows a large symmetry with respect to intensity, horizontal pattern, and BF elements [76].

In the TAV, we can identify both mechanical and thermodynamic processes, and their relative contribution is still a matter of discussion. While, in general, it is widely accepted that the BF, a largely mechanical process, is responsible for the development of the Atlantic Niño mode, some recent studies point out that thermodynamic processes play a vital role for the evolution of this mode. For example, ref. [79] found in an ensemble of multi-CGCM simulations that thermodynamics plays the leading role in the development of the Atlantic Zonal Mode. According to their results, thermodynamic processes, mainly through the surface latent heat flux, drive the Atlantic Niño mode and the related mechanism is consistent with a first-order autoregressive process. They claim that the weakening of the equatorial trade winds (associated with the activity of SAA) leads to the reduction of the release of surface latent heat flux two months earlier than the typical Atlantic Niño events and this suppresses the heat flux which induces the warm SST anomaly. In contrast, other modeling and observational studies discuss that the role of thermodynamic processes in the TAV is mainly damping the SST anomalies and that are those who induce the surface heat flux anomalies (e.g., [73,76]). In particular, in [72] it is pointed out that the SST bias of a coupled model leads to an unrealistic thermodynamic positive role in the TAV.

The aforementioned dynamical and thermodynamic processes responsible for the evolution of the TAV take place in the equatorial region. However, it has been suggested that off-equator processes can substantially influence the initiation and development of the TAV. For instance, [80] showed that in some of the Atlantic Niño events, the SST anomalies were generated north of the equator and are advected meridionally by the ocean currents to the equator. Not only the surface, but the subsurface equatorial Atlantic Ocean can be important for the TAV: vertically alternating deep zonal jets of short vertical wavelength propagate their energy upward to the surface, connecting with surface zonal current anomalies and eastern equatorial Atlantic temperature anomalies [81]. On the other hand, the westward propagating Rossby waves reflect at the western boundary of the equatorial Atlantic. This reflecting wave travels as Kelvin waves eastward and consequently contributes to the onset of the Atlantic Niño/Niña events [82–84]. An even more important off-equator contributor to the Atlantic Niño mode is South Atlantic Anticyclone. Ref. [64] showed that in observations and reanalysis data the winter-to-spring (February–March) SAA variability is highly correlated with the summer (June–July) Atlantic Niño mode. Moreover, [85] suggested that the SAA variability is transferred to the Atlantic

Niño mode via anomalous tropical wind power: stronger SAA activity in February leads to an earlier onset and further amplification of the ACT in summer (Atlantic Niña condition) and weaker SAA delays the development of the ACT summer, resulting in Atlantic Niño. This connection between the SAA and Atlantic Niño Mode can demonstrate a relationship between Atlantic Niño Mode and the Benguela Niño Mode since the Benguela upwelling system is maintained by the Benguela low-level jet associated with the SAA (e.g., [86–88]). These nonlocal features for the Atlantic Niño modes are not found in the El Niño modes in the tropical Pacific. The discussion of the association between the Atlantic Niño mode and the Benguela Niño mode will be later in the text.

One of the largest impacts of the Atlantic Niño Mode is exerted on the Intertropical Convergence Zone (ITCZ). In summer, when the Atlantic Niño mode usually reaches its peak, the climatological ITCZ is sitting in the north of the equator due to the West African Monsoon (WAM). At basin-scale, the WAM is driven by the land–ocean temperature contrast between the African Continent and the South Atlantic Ocean. However, at a regional scale, this climatological large-scale temperature gradient is changed by a well-developed ACT, and the magnitude of the ACT anomalies contributes to the location of the ITCZ and intensity of the WAM (e.g., [51,53,54]). Over the ACT, cumulus convection is inhibited because of reduced atmospheric instability due to the colder SST (about 24 °C), according to the relationship between tropical marine precipitation and underlying SST (e.g., [89–91]). The climatological land–sea contrast is modified by the Atlantic Niño mode as shown in Figure 6. The precipitation associated with the ITCZ is correlated positively to a large extent with the Atlantic Niño mode. Not only the equatorial Atlantic, but also the western coastal African and South American countries are influenced by the AZM [22]: north of the equator (5–10° N), a negative correlation of precipitation is found, indicating that the ITCZ is displaced southward following the Atlantic Niño/Niña. The wind stress is also well correlated to the AZM: the wind stress converges over the Atlantic 3 region (20° W–0°, [85]) and a westerly (easterly) anomaly is detected over the western equatorial Atlantic (Gulf of Guinea) showing the resemblance of the first element of BF (Figure 5a). Additionally, the WAM is weakened, reinforced by the Atlantic Niño/Niña over the Gulf of Guinea to the coastal region.

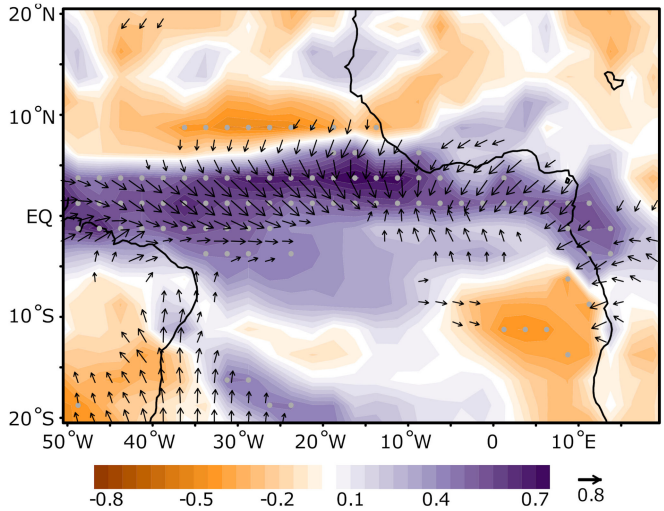

Figure 6. Correlation map between PC1 score and precipitation (color, GPCP, 1979–2015) and wind stress (vector, ERA-Interim, 1979–2011) in June. The gray dots denote 95% significance level.

4.3. Atlantic Meridional Mode

The Atlantic Meridional Model (AMM), the second fundamental mode of the tropical Atlantic variability, is captured as the second EOF of the monthly SST anomalies, as shown in Figure 7a. The AMM has an interhemispheric dipole structure (e.g., [21,82]) opposite to the AZM, which has an L-shaped peak in the Gulf of Guinea, as seen in Figure 2a. The AMM appears frequently in boreal spring (April to May) as shown by the PC of 2nd EOF mode in Figure 7b. The main mechanism for

the generation and maintenance of the AMM is the so-called wind-evaporation–SST (WES) feedback (e.g., [92,93]). It also encompasses air–sea interactions, but the mechanisms responsible for the AZM are different: during the negative phase of AMM, as shown in Figure 7a, negative SST anomalies are seen in the North tropical Atlantic and positive SST anomalies in the South tropical Atlantic. Corresponding to these SST anomalies, the sea level pressure (SLP) anomalies are positive and negative over the North and South tropical Atlantic, respectively. The interhemispheric SLP dipole pattern drives the surface wind anomalies, as shown in Figure 6, blowing from the North to South tropical Atlantic. Over the north of the equator, this surface wind anomaly enhances the easterly trade winds. In contrast, south of the equator, the trade winds are decelerated. These surface wind anomalies induce the positive and negative (upward is positive) latent heat flux over the north and south tropical Atlantic anomalies in Figure 8a. Consequently, the original SST anomalies are excited by the wind-driven evaporation anomalies. The AMM also influences the ITCZ over the equatorial Atlantic: during the negative phase of the AMM, the southerly surface wind anomalies result in a southward shift of the ITCZ as shown in Figure 8b.

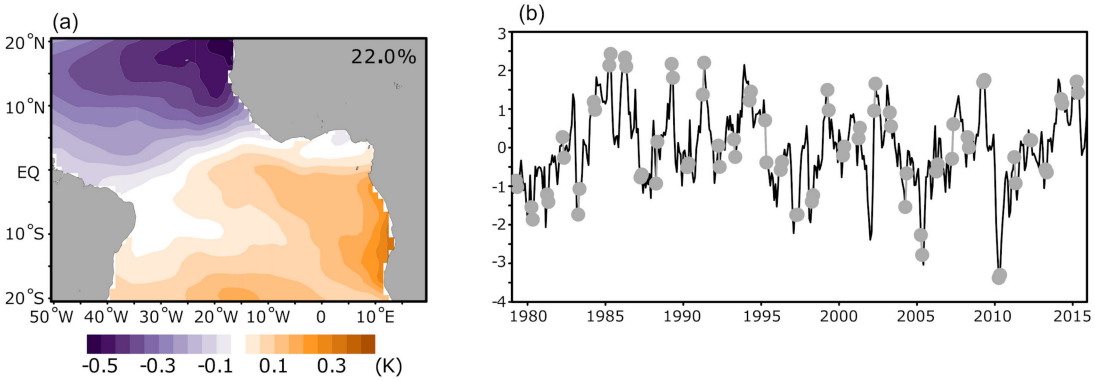

Figure 7. Same as Figure 4, but for EOF 2nd mode (**a**) and gray dots denote the PC score in April and May for each year (**b**).

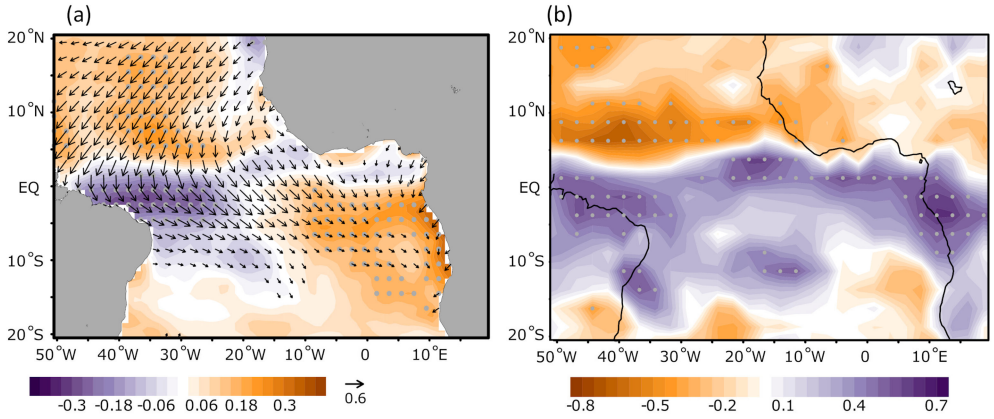

Figure 8. (**a**) Correlation map between PC2 score and latent heat flux (color, TropFlux, 1979–2015, upward is positive) and surface wind stress (vector, ERA-Interim, 1979–2011). The gray dots denote 99% significance level and vector is only shown with 99% significance level. (**b**) same as Figure 4, but for correlation of precipitation with PC2 score in May.

4.4. Benguela Niño/Niña

The strong interannual variability in the ABF, by similarity with the variability in the ATC, is named Benguela Niño/Niña. The ABF variability has its peak amplitude in boreal spring (March to April, e.g., [94]) as shown in Figure 3c. Even though the spatial distribution of the Benguela Niño/Niña is limited, its influence on the local and regional weather/climate is not negligible. [95]

showed that the Benguela Niños (warm event) enhances the precipitation over the coastal regions of Angola and Namibia, and attributed this increase in precipitation to an associated anomalous moisture flux convergence. Ref. [23] suggested that the Benguela Niño amplifies the moisture flux toward the African continent, reaches the eastern coast of South Africa and consequently, the mesoscale convective system is enhanced by the moisture flux due to the Benguela Niño in January, 2013.

The origin of the Benguela Niño/Niña is still disputed by several studies. One possible mechanism is local wind forcing (e.g., [96,97]). According to this hypothesis, the Angola–Benguela Frontal Zone is maintained mainly by the tilting effect due to the upwelling and meridional confluence effect of the Angola and Benguela Currents (see Figure 1 of this manuscript; see also [10]). Both frontogenetic terms are related to the local wind stress forcing. Ref. [9,98,99] showed that the location of the Angola–Benguela Frontal Zone is sensitive to the local wind stress curl. In refs. [100] and [35] it was concluded that the anomalous negative wind stress curl over the frontal region, inducing the southward penetration of the Angola Current transporting the warm water from the tropics and consequently, the warm SST bias (similar situation as Benguela Niño) is generated in coupled models.

Another possible mechanism is a remote excitation from the equatorial Atlantic via Kelvin waves (e.g., [64,69,94,101,102]). According to this, the zonal wind stress anomaly over the western equatorial Atlantic forces the downwelling Kelvin waves to propagate eastward and along the West African coast. These Kelvin waves continuously travel southward. Consequently, these downwelling anomalies deepen the thermocline in the Angola–Benguela Frontal Zone and the warm SST anomalies are generated. This mechanism is indicated in Figure 5 for the Bjerknes Feedback for the AZM. The signal of the wind-forced Kelvin waves extends from the equatorial Atlantic to the Angola–Benguela Frontal Zone (Figure 3b) and SST anomalies are highly related to the sea-surface height (thermocline depth) anomalies in the front area.

Those arguments indicate a tight linkage between the AZM and Benguela Niño/Niña. In ref. [64] it was shown that the Benguela events lead the AZM by a few months via variability in the SAA. Figure 9 gives lag-composite anomalies of SST and SLP obtained from observations and reanalysis data for Atlantic Niño and Niña cases in June. The Atlantic Niño and Niña are defined as the Atlantic 3 index larger and smaller than one standard deviation of Atlantic 3 index. In February, the most pronounced SST anomalies are located in the south Atlantic and weak SST anomalies in the equatorial Atlantic in both events. Noticeably, the negative and positive SLP anomalies are found around 30° S in warm and cold events, respectively. From March to April, the SLP anomalies become larger over the South Atlantic. Interestingly, the strong SST anomalies in the Angola–Benguela Frontal Zone are generated in both cases. On the other hand, the SST anomalies in the equatorial Atlantic develop gradually in spring. From May to June, the SLP anomalies over the South Atlantic disappear. The SST anomalies in the equatorial Atlantic are maximized and consequently, Atlantic Niño and Niña are generated in summer. This result is consistent with [52] and indicates that the spring Benguela Niño/Niña are tightly connected to the summer Atlantic Niño/Niña and its connection could be made by the SAA. However, the question about the mechanism how the SAA variability initiates the evolution of the Atlantic Niño/Niña is still open. For instance, it has been proposed that these may be associated with a southward position of the intertropical convergence zone (ITCZ). This culminates in the generation of the so-called double ITCZ in boreal summer, driving an excessive precipitation from about 5° S to 10° S.

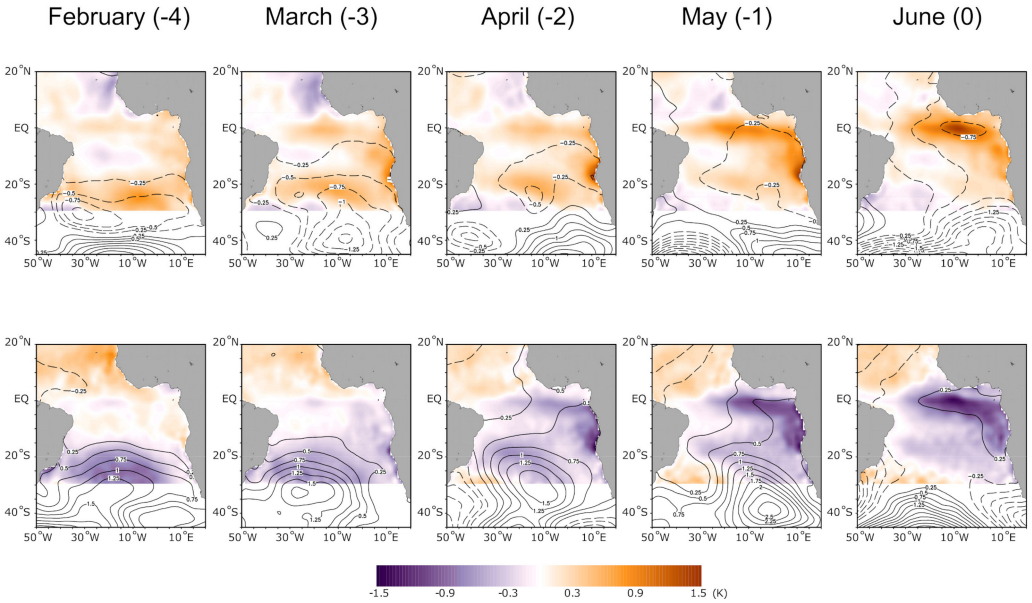

Figure 9. Lagged-composite SST (color) and sea level pressure (contour) for (first row) warm and (second row) cold events for the observations (TropFlux and ERA-Interim for 1980–2010). The events are defined as detrended monthly ATL3 index anomalies that are higher and lower than one standard deviation of ATL3 index in June. Lagged composites are examined from February to June.

5. Variability at Longer Time Scales

The TA also features an important variability at longer time scales which may be related to either external forcings or internal variability (see e.g., [4]). Ref. [103] identified a surface warming during the past six decades that is associated with a weakened AZM interannual variability. This warming is greater in the eastern equator. They hypothesized that enhanced warming to the east leads to greater atmospheric convection in the eastern equatorial basin, as well as to weakened trade winds. The wind slackening to the east deepens the thermocline and leads to a stronger warming. The flattened thermocline reduces the AZM variability by a reduction of thermocline feedback. They suggested that these changes could be related to anthropogenic aerosols. However, the observed low-frequency variability could also be associated with changes in the global ocean circulation, which manifests through the AMOC variability or to the influence of the variability in higher latitudes and/or other basins [104]. Low-frequency changes in the TAV are reflected in changes in the background state of the ocean [105] and in the spatial structure of the AZM [106].

The changes in the AZM spatial pattern are accompanied by variations in its periodicity, explained variance and regional impacts [105,106]. Of special relevance is the shift in the AZM behavior that took place in the 1970s, when the positive SST anomalies that characterized the AZM changed to a more basin-wide pattern, with positive anomalies covering the entire equatorial Atlantic. In the work by [106] it is argued that the change in AZM characteristics impacted the AZM-ENSO teleconnection: before the 1970s, the subsidence over the Maritime Continent produced by the Atlantic Niño was strong enough to counteract the impact of the Pacific Walker circulation on surface winds, thus precluding the teleconnection to occur. The change of the AZM spatial pattern and teleconnections could be explained by the modulation by large-scale, low-frequency variability modes. Changes in the global background state and the alteration of atmospheric teleconnections could cause the diversity of AZM patterns and impacts along the observational record. However, these interpretations should be taken with caution. The short observational period available (~100 years) does not rule out that they are a reflection of internal variability. It is also possible that low-frequency variability changes the frequency of occurrence of different types of variability in the AZM: [107] found in a GCM simulation that, similarly

to ENSO [108], different kinds of Atlantic Niño events can be identified and that their teleconnections to ENSO are of a different nature.

Of especial importance is the teleconnection with the tropical Pacific: the TA influences the Tropical Pacific variability, in particular its strongest manifestation, ENSO, and vice-versa. This connection is modulated by the Atlantic Multidecadal Oscillation (AMO) and involves both AZM and AMM modes of variability [109]. The connection of the Tropical Pacific with the AZM is more active during AMO negative phases [110,111], when the eastern equatorial Atlantic SST variability is enhanced due to a shallower thermocline there [105]. According to [28], positive (negative) AZM events favor the development of negative (positive) ENSO events through the strengthening (weakening) of the Walker circulation. The resulting enhanced surface divergence in the central Pacific shallows (deepens) the equatorial thermocline triggering coupled processes, and favoring the development of a negative (positive) ENSO event.

ENSO is also affected by the AMM [109]: cooling in the North TA during boreal spring generates a low-level anticyclonic flow over the eastern Pacific. On the western flank of this anticyclonic flow, reduced wind speed and warm wet moist energy advection due to the southerly lead to SST warming with enhanced convective activity in the following winter. Moreover, Wang et al. (2017) identify an Atlantic capacitor mechanism according to which ENSO influences the North TA via an atmospheric bridge ("charging") and in turn, the NTA triggers the following ENSO via a subtropical teleconnection ("discharging", according to [109]. This feedback from the Atlantic North TA to ENSO, which enhances the variability in the Pacific, is stronger in the positive phase of the AMO and has been active since the early 1990s thanks to a more favorable background state provides by the positive phase of the AMO and global warming.

The variability and the teleconnections associated to the AZM and AMM can change in the future climate. For instance, ref. [112] found that projected warmer SSTs cause a modification of the influence of the AZM on the Tropical Atlantic rainfall, the Asian monsoon, and the land surface temperature in the extratropics, even when the AZM characteristics remains unchanged. In [113] it was found that the doubling of atmospheric CO2 leads to a northward shift of the ITCZ in summer and fall and to a damping of evaporation anomalies that weakens the WES feedback in the northern TA. This reduction of WES feedback in the northern TA leads to a weakening of the AMM.

The changes in the TA variability modes caused by global warming would also affect the strength of the relationship between the TAV and the tropical Pacific, where the Atlantic warming could cause a reduction of the warming in the eastern tropical Pacific through modification of the Walker circulation. These changes cause easterly surface wind anomalies in the central-west Pacific which are amplified by coupled ocean–atmosphere processes [114]. The influence of the North TA on ENSO could be modulated by the strength of the TA warming [115]. The modification of the TA–Tropical Pacific teleconnection could also influence the frequency of strong ENSO events [116] and the occurrence of different kinds of ENSO events [109].

A clear decadal variability signal can also be identified in the SETA region. For instance, ref. [117] found, in the last decades, a southward latitudinal shift of the annual mean ABFZ position and a reinforcement of the associated meridional temperature gradient. These changes are associated with warming (cooling) of the ocean mixed layer temperatures equatorward (poleward) of the front over the 1980–2014 period. They argued that oceanic cooling poleward of the ABFZ is primarily due to enhanced advection of cooler water from the south and east, increased cooling by vertical diffusion, and shoaling of the mixed-layer depth. In the atmosphere, these changes are related to an intensification and a poleward shift of the South Atlantic subtropical anticyclone, hence the westward mixed layer ocean currents intensify in the Benguela upwelling region along the Namibian coast. These results could point to a role of changes in the oceanic circulation and the air/sea interactions mechanisms proposed by [61].

6. Modeling the Climate of the TA

Numerical models of different resolution and complexity have been used to gain insight into long-term and decadal patterns and its variability, as well as for medium- and short-term prediction of TA. Among them, Global Coupled Models (GCMs) are the most sophisticated tool, as they provide a state-of-the-art description of climate [118]. Whilst the ability of coupled atmosphere–ocean general circulation models to simulate the observed climate and its variability has improved over the last few years, they still present strong differences with respect to observations. As the biases in the simulations reduce our confidence in the use of climate predictions and projections delivered by current GCMs for the Tropical Atlantic basin and adjacent regions, the scientific community, with the special contribution of the CMIP, has made a special effort to improve model performance in the Tropical Oceans. This effort culminated in a reduction of SST biases in the Tropical Pacific, but not much progress has been done in the reduction of SST biases in the Tropical Atlantic [119].

GCMs generally overestimate the SSTs in the tropics (e.g., [100,120,121], where large SST biases in the ACT constitute a major problem to realistically simulate rainfall provided by the Western African Monsoon in present-day and future climates [122]. These biases have a marked seasonality, becoming stronger in boreal summer and fall and reach their maximum in November–December [123]. However, biases are largest in the eastern boundary of the TA, in the SETA region (see for instance, Figure 10, which shows the biases for the AWI-CM coupled model). In this area, warm coastal biases in the individual models that contribute to CMIP5 reach even more than 5 °C [119]. Also, precipitation in current GCMs presents an excessively symmetric structure across the equator [120,124,125], resulting in double ITCZ. Consistently with these rainfall biases, models also show errors in the simulation of upper-tropospheric clouds in the tropics [126].

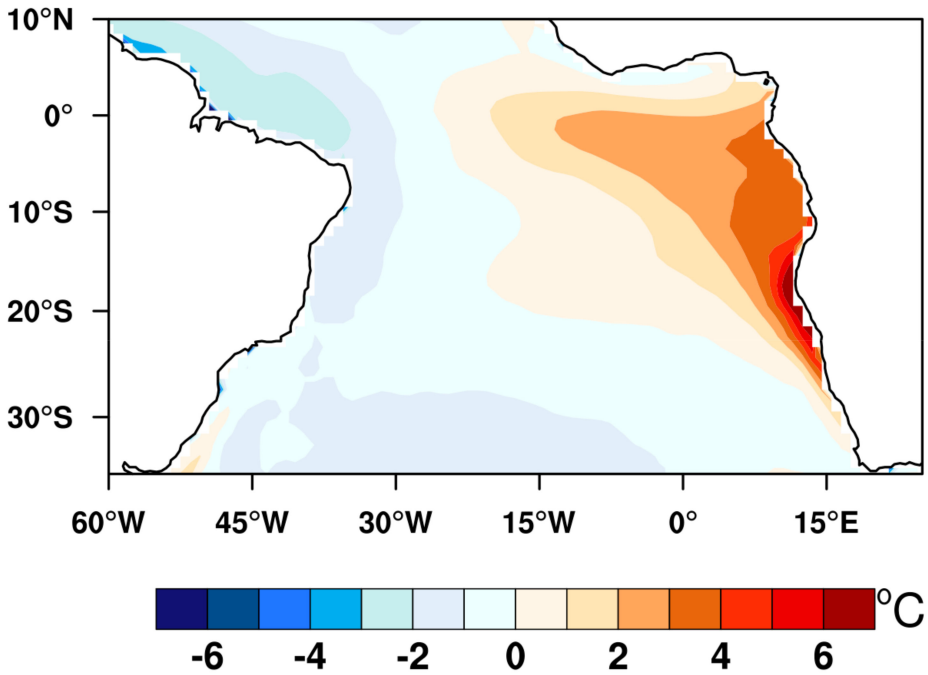

Figure 10. Mean SST bias for the 1988–2007 period in a present time simulation with the coupled global model AWI-CM.

The causes for these systematic biases in the simulated TAV have been intensively examined and they are strongly model dependent. Overall, warm errors are can be, roughly speaking, related to (i) drawbacks in the physics of the ocean and atmospheric models and (ii) insufficient model resolution in the horizontal and/or vertical coordinates of the individual atmospheric and oceanic components of the coupled model [119,127,128]. A systematic drawback shared by many state-of-the-art

coupled models is an underestimation of coastal upwelling [121]. This has been generally attributed to a spurious weakening of the northward Benguela Current, as well as to an underestimation of the strength of the Benguela low-level jet [87,88]. It has also been proposed that, even when the simulated upwelling intensity is well captured, the misrepresentation of the sharp thermocline characteristic of the TA culminates in upwelling of waters which are warmer than observed, therefore contributing to coastal SST biases [34,129]. In turn, the simulated southward Angola Current tends to be stronger than in observations due to an excessive negative wind stress curl in the near shore [91,130]. The misrepresentation of this near-current system, with the implied strengthening (weakening) of the Angola Current (Benguela Current) results in a southward migration of the ABF [131]. Observations indicate that the ABF is positioned close to 16° S [132], whilst in the CMIP5 ensemble mean, the convergence area is displaced to the south by about 10°. Another major source of warm SST biases is sustained by an excessive shortwave radiative flux into the ocean due to an underestimation of low marine stratiform clouds over the SETA [133–135]. Along with this, a deficient surface evaporation due to an overestimation of near-surface humidity by the atmospheric component of GCMs within the eastern TA has also been found to be a driver of SST biases [136].

The biased SST in the TA is not only driven by these local factors, but can also be provoked by remote forcings via teleconnections. For instance, westerly wind biases in the equatorial TA leads to a spurious shoaling of the thermocline to the west, and a deepening of the thermocline to the east [36,137,138] and this hampers the development of the Atlantic Cold Tongue [80]. The resulting equatorial warm biases are subsequently advected along the equatorial strip and to the SETA via Kelvin waves [36,139]. The existence of the westerly wind bias and associated errors in wind stress in the equator can be a consequence of several factors, such as the underrepresentation of zonal momentum flux across the top of the boundary layer [140] and/or excessive (deficient) rainfall over equatorial Africa (South America) with insufficient lower-tropospheric diabatic heating over the Amazon [141]. The simulation of artificial barrier layers in the southeastern equatorial Atlantic could also hinder the development of the cold tongue, contributing to the local warm SST bias [142]. Although the ultimate reasons for the tropical Atlantic SST biases might be model dependent, the positive feedbacks between wind stress, clouds, and SSTs seem to be key for maintaining and even enhancing the biases [34].

Recent results show that the biases can also be of remote origin. For instance, an incorrect simulation of low-marine cloud cover in the southeastern tropical Pacific and Atlantic Oceans and in the Southern Ocean affect the simulated position of the ITCZ, impacting the TAV [143]. Also, an incorrect simulation of global circulation can affect the simulation of the SETA climate, as a weak Atlantic meridional overturning circulation (AMOC; [144]) seems to be associated to a warm SETA bias. Also, failures in the representation of the South Atlantic Anticyclone south of 20° S [34] and an incorrect representation of the Agulhas leakage [129] could be important contributors to the warm bias in the tropical Atlantic. Also, the authors of [145] found that cloud biases in the Southern Ocean could be accountable for a large part of the double ITCZ bias.

A great effort has been devoted to unraveling the role of atmospheric and oceanic resolutions in the representation of the TA climate, although there is not a clear consensus regarding this topic. While some works claim that increasing the model resolution reduces warm biases notably (e.g., [146,147]), other studies conclude that biases are only alleviated to a small extent in response to an increased model resolution (e.g., [133,148]). This may be related to the fact that, in many studies, a simultaneous increase of both oceanic and atmospheric model components is carried out. Besides changes in the oceanic resolution in the compared runs, other parameterizations that could also affect the results obtained are generally also performed. Ref. [146] argued that the use of an eddy-resolving ocean model results in an improved simulation of coastal Benguela upwelling system which, in turn, lowers coastal biases in the near shore. In the work by [130] it is shown that the combination of an eddy-resolving ocean model and an atmospheric model with a nominal resolution of at least 0.5° is needed to realistically simulate the Benguela upwelling system. The authors further claimed that this atmospheric resolution is required for a better representation of the simulated wind stress curl near the African coast. In line with this, the

model study of [149] highlighted that near-shore wind affects the representation of near-surface eastern boundary currents and this has a concomitant impact on the SST. Regarding the vertical resolution of the models, in ref. [147] it is concluded that an important reduction of warm biases in the TA occurs when the horizontal and vertical resolution of the atmospheric model are simultaneously refined.

7. Conclusions and Outlook

The improvement of our understanding of the TAV is important from the scientific point of view due to the impact that this variability has on the climate of Eastern South America and Western Africa, as well as due to the connections between the climate tropical Atlantic and the Pacific. The question also has societal and environmental implications, as the TAV influences the marine and land ecological systems in the Atlantic and this has a significant impact on the societies of the implied countries. This improvement should be based both on a better observing system and climate models. In [5], a good discussion of the necessary steps for the improvement of the observing system can be found. As the climate simulated by global coupled models still presents significant biases, the improvement of the data assimilation techniques and the numerical models used for the generation of reanalysis is also desirable. In this regard, the development of coupled systems for forecast and reanalysis looks very promising. In view of the strengths and weaknesses of state-of-the-art coupled models to simulate the climate variability of the TA, it is clear that the modeling community still has to face important challenges. Presently, model resolution continues to be a limitation for the available computational resources. Higher horizontal resolution of the corresponding atmospheric and oceanic components can have a positive impact on the simulation of the TA climate. On one hand, an increased atmospheric resolution will allow a better representation of wind stress curl near the African coast. This, in turn, will lead to an improved simulation of the Angola and Benguela currents. On the other hand, a refinement in the horizontal resolution of the oceanic component (to ~5–10 km) will improve the representation of the mesoscale ocean circulation associated with strong coastal currents and will drive an intensification of the Benguela upwelling system. Both will contribute to a reduction of SST warm biases in the SETA. In this regard, a new generation of oceanic models on unstructured grids (see e.g., [150]) brings the possibility of running climate simulations at eddy-resolving resolutions in the ocean component with acceptable computational costs. The SST equatorial biases are related to the equatorial westerly wind bias in March–May, which deepens the thermocline and inhibits cooling during the subsequent June–August upwelling season [33,141], pointing to the role of the atmospheric model in bias generation. As shown by [147], an enhanced horizontal and vertical atmospheric resolution contributes to alleviate these biases. Another factor that may contribute to the cold tongue bias relates to deficiencies in vertical mixing parameterizations that lead to problems in the representation of the oceanic thermocline [100].

Also important is the question of the relative importance of the dynamics and the thermodynamical forcing for the generation of the biases in SETA. Another feature of concern regards the achievement of an improved simulation of the ITCZ [124,125]. The Atlantic ITCZ simulated by current models is usually shifted southward. Although this shift is exacerbated by the coupling, this is already present in atmosphere-only simulations [151]. This shift is probably caused by an incorrect simulation of stratocumulus clouds. Another possible cause is a weak AMOC, which generates a cold SST bias in the North Atlantic and warm bias in the Atlantic cold tongue [152].

Funding: Work conducted by William Cabos and Alba de la Vara has been funded by the Spanish Ministry of Science, Innovation and Universities, the Spanish State Research Agency and the European Regional Development Fund, through grant CGL2017-89583-R. William Cabos has also been supported by Salvador Madariaga grant (Spanish Ministry of Science Innovation and Universities). S. Koseki has been supported by Giner de los Rios 2018/19 (University of Alcalá) and STERCP (European Research Council, grant no. 648982).

Acknowledgments: We are grateful to Elva Wang for efficiently handling the review process. We thank both anonymous reviewers for their insightful comments, which allowed us to improve this manuscript.

Conflicts of Interest: The authors declare no conflict of interest.

References

1. Xie, S.P.; Carton, J.A. Tropical Atlantic variability: Patterns, mechanisms, and impacts. In *Earth's Climate: The Ocean–Atmosphere Interaction*; American Geophysical Union: Washington, DC, USA, 2004; Volume 147, pp. 121–142.
2. Muñoz, E.; Weijer, W.; Grodsky, S.A.; Bates, S.C.; Wainer, I. Mean and variability of the tropical Atlantic Ocean in the CCSM4. *J. Clim.* **2012**, *25*, 4860–4882. [CrossRef]
3. Tourre, Y.M.; Rajagopalan, B.; Kushnir, Y. Dominant patterns of climate variability in the Atlantic Ocean during the last 136 years. *J. Clim.* **1999**, *12*, 2285–2299. [CrossRef]
4. Lübbecke, J.F.; Rodriguez-Fonseca, B.; Richter, I.; Martin-Rey, M.; Losada, T.; Polo, I.; Keenlyside, N.S. Equatorial Atlantic variability-Modes, mechanisms, and global teleconnections. *Wiley Interdiscip. Rev. Clim. Chang.* **2018**, *9*, e527. [CrossRef]
5. Foltz. The Tropical Atlantic Observing System. Frontiers in Marine Science. 2019. Available online: https://doi.org/10.3389/fmars.2019.00206 (accessed on 08 June 2019).
6. Bourlès, B.; Araujo, M.; McPhaden, M.J.; Brandt, P.; Foltz, G.R.; Lumpkin, R.; Giordani, H.; Hernandez, F.; Lefèvre, N.; Nobre, P.; et al. PIRATA: A Sustained Observing System for Tropical Atlantic Climate Research and Forecasting. *Earth Space Sci.* **2019**, *6*, 577–616. [CrossRef]
7. Dippe, T.; Krebs, M.; Harlaß, J.; LübbeckeM, J.F. Can Climate Models Simulate the Observed Strong Summer Surface Cooling in the Equatorial Atlantic. In *YOUMARES 8—Oceans Across Boundaries: Learning from Each Other*; Jungblut, S., Liebich, V., Bode, M., Eds.; Springer: Berlin, Germany, 2018.
8. Weingartner, T.J.; Weisberg, R.H. A description of the annual cycle in sea surface temperature and upper ocean heat in the equatorial Atlantic. *J. Phys. Oceanogr.* **1991**, *21*, 83–96. [CrossRef]
9. Colberg, F.; Reason, C.J.C. A model study of the Angola–Benguela Frontal Zone: Sensitivity to atmospheric forcing. *Geophys. Res. Lett.* **2006**, *33*, L19608. [CrossRef]
10. Koseki, S.; Giordani, H.; Goubanova, K. Frontogenesis of the Angola–Benguela Frontal Zone. *Ocean. Sci.* **2019**, *15*, 83–96. [CrossRef]
11. Wainer, I.; Soares, J. North northeast Brazil rainfall and its decadal-scale relationship to wind stress and sea surface temperature. *Geophys. Res. Lett.* **1997**, *24*, 277–280. [CrossRef]
12. Xie, S.P. On the genesis of the equatorial annual cycle. *J. Clim.* **1994**, *7*, 2008–2013. [CrossRef]
13. Chang, P.; Philander, S.G. Coupled ocean–atmosphere instability of relevance to the seasonal cycle. *J. Atmos. Sci.* **1994**, *51*, 3627–3648. [CrossRef]
14. Nigam, S.; Chao, Y. Evolution dynamics of tropical ocean–atmosphere annual cycle variability. *J. Clim.* **1996**, *9*, 3187–3205. [CrossRef]
15. Li, T.; Philander, S.G.H. On the annual cycle of the eastern equatorial Pacific. *J. Clim.* **1996**, *9*, 2986–2998. [CrossRef]
16. Czaja, A.; Van der Vaart, P.; Marshall, J. A diagnostic study of the role of remote forcing in tropical Atlantic variability. *J. Clim.* **2002**, *15*, 3280–3290. [CrossRef]
17. Ruiz-Barradas, A.; Carton, J.A.; Nigam, S. Structure of interannual-to-decadal climate variability in the tropical Atlantic sector. *J. Clim.* **2000**, *13*, 3285–3297. [CrossRef]
18. Enfield, D.B.; Mayer, D.A. Tropical Atlantic sea surface temperature variability and its relation to El Niño-Southern Oscillation. *J. Geophys. Res. Oceans* **1997**, *102*, 929–945. [CrossRef]
19. Zebiak, S. Air–sea interaction in the equatorial Atlantic region. *J. Clim.* **1993**, *6*, 1567–1586. [CrossRef]
20. Polo, I.; Rodríguez-Fonseca, B.; Losada, T.; García-Serrano, J. Tropical Atlantic variability modes (1979–2002). Part I: Time-evolving SST modes related to West African rainfall. *J. Clim.* **2008**, *21*, 6457–6475. [CrossRef]
21. Chiang, J.C.; Vimont, D.J. Analogous Pacific and Atlantic meridional modes of tropical atmosphere–ocean variability. *J. Clim.* **2004**, *17*, 4143–4158. [CrossRef]
22. Lutz, K.; Jacobeit, J.; Rathmann, J. Atlantic warm and cold water events and impact on African west coast precipitation. *Int. J. Clim.* **2015**, *35*, 128–141. [CrossRef]
23. Manhique, A.J.; Reason, C.J.C.; Silinto, B.; Zucula, J.; Raiva, I.; Congolo, F.; Mavume, A.F. Extreme rainfall and floods in southern Africa in January 2013 and associated circulation patterns. *Nat. Hazards* **2015**, *77*, 679–691. [CrossRef]
24. Nobre, P.; Shukla, J. Variations of sea surface temperature, wind stress, and rainfall over the tropical Atlantic and South America. *J. Clim.* **1996**, *9*, 2464–2479. [CrossRef]

25. Vimont, D.J.; Kossin, J.P. The Atlantic meridional mode and hurricane activity. *Geophys. Res. Lett.* **2007**, *34*, 7. [CrossRef]
26. Doi, T.; Tozuka, T.; Yamagata, T. The Atlantic Meridional Mode and Its Coupled Variability with the Guinea Dome. *J. Clim.* **2010**, *23*, 455–475. [CrossRef]
27. Kucharski, F.; Bracco, A.; Yoo, J.H.; Molteni, F. Atlantic forced component of the Indian monsoon interannual variability. *Geophys. Res. Lett.* **2008**, *35*. [CrossRef]
28. Rodríguez-Fonseca, B.; Polo, I.; García-Serrano, J.; Losada, T.; Mohino, E.; Mechoso, C.R.; Kucharski, F. Are Atlantic Niños enhancing Pacific ENSO events in recent decades? *Geophys. Res. Lett.* **2009**, *36*. [CrossRef]
29. Barichivich, J.; Gloor, E.; Peylin, P.; Brienen, R.J.W.; Schongart, J.; Espinoza, J.C.; Pattnayak, K.C. Recent intensification of Amazon flooding extremes driven by strengthened Walker circulation. *Sci. Adv.* **2018**. [CrossRef] [PubMed]
30. Losada, T.; Rodriguez-Fonseca, B.; Mohino, E.; Bader, J.; Janicot, S.; Mechoso, C.R. Tropical SST and Sahel rainfall: A non-stationary relationship. *Geophys. Res. Lett.* **2012**, *39*. [CrossRef]
31. Losada, T.; Rodríguez-Fonseca, B.; Kucharski, F. Tropical influence on the summer Mediterranean climate. *Atm. Sci. Lett.* **2012**, *13*, 36–42. [CrossRef]
32. Jin, D.; Huo, L. Influence of tropical Atlantic sea surface temperature anomalies on the East Asian summer monsoon. *Q. J. R. Meteorol. Soc.* **2018**, *144*, 1490–1500. [CrossRef]
33. Richter, I.; Xie, S.P. On the origin of equatorial Atlantic biases in coupled general circulation models. *Clim. Dyn.* **2008**, *31*, 587–598. [CrossRef]
34. Cabos, W.; Sein, D.V.; Pinto, J.G.; Fink, A.H.; Koldunov, N.V.; Alvarez, F.; Izquierdo, A.; Keenlyside, N.; Jacob, D. The South. Atlantic as a key player for the representation of the tropical Atlantic climate in coupled climate models. *Clim. Dyn.* **2017**, *48*, 4051–4069. [CrossRef]
35. Koseki, S.; Keenlyside, N.; Demissie, T.; Toniazzo, T.; Counillon, F.; Bethke, I.; Ilicak, M.; Shen, M.-L. Causes of the large warm bias in the Angola–Benguela Frontal Zone in the Norwegian Earth System Model. *Clim. Dyn.* **2018**, *50*, 4651–4670. [CrossRef]
36. Goubanova, K.; Sanchez-Gomez, E.; Frauen, C.; Voldoire, A. Respective roles of remote and local wind stress forcings in the development of warm SST errors in the South-Eastern Tropical Atlantic in a coupled high-resolution model. *Clim. Dyn.* **2019**, *52*, 1359–1382. [CrossRef]
37. Jayne, S.R.; Roemmich, D.; Zilberman, N.; Riser, S.C.; Johnson, K.S.; Johnson, G.C.; Piotrowicz, S.R. The Argo Program: Present and future. *Oceanography* **2017**, *30*, 18–28. [CrossRef]
38. Zilberman, N.V.; Roemmich, D.H.; Gille, S.T. The East Pacific Rise current: Topographic enhancement of the interior flow in the South Pacific Ocean. *Geophys. Res. Lett.* **2017**, *44*, 277–285. [CrossRef]
39. Schott, F.A.; Dengler, M.; Zantopp, R.; Stramma, L.; Fischer, J.; Brandt, P. The Shallow and Deep Western Boundary Circulation of the South Atlantic at 5°–11°S. *J. Phys. Oceanogr.* **2005**, *35*, 2031–2053. [CrossRef]
40. Hummels, R.; Brandt, P.; Dengler, M.; Fischer, J.; Araujo, M.; Veleda, D.; Durgadoo, J.V. Interannual to decadal changes in the western boundary circulation in the Atlantic at 11 degrees S. *Geophys. Res. Lett.* **2015**, *42*, 7615–7622. [CrossRef]
41. Kopte, R.; Brandt, P.; Claus, M.; Greatbatch, R.J.; Dengler, M. Role of equatorial basin-mode resonance for the seasonal variability of the angola current at 11 degrees S. *J. Phys. Oceanogr.* **2018**, *48*, 261–281. [CrossRef]
42. Send, U.; Lankhorst, M.; Kanzow, T. Observation of decadal change in the Atlantic meridional overturning circulation using 10 years of continuous transport data. *Geophys. Res. Lett.* **2011**, *38*, L24606. [CrossRef]
43. Frajka-Williams, E.; Lankhorst, M.; Koelling, J.; Send, U. Coherent circulation changes in the deep north atlantic from 16 degrees N and 26 degrees N transport arrays. *J. Geophys. Res. Ocean.* **2018**, *123*, 3427–3443. [CrossRef]
44. Yu, L. Sea surface exchanges of momentum, heat, and freshwater determined by satellite remote sensing. In *Encyclopedia of Ocean Sciences*; Cochran, J.K., Bokuniewicz, H.J., Yager, P.L., 3rd, Eds.; Academic Press: Cambridge, MA, USA, 2018.
45. Saha, S.; Moorthi, S.; Wu, X.; Wang, J.; Nadiga, S.; Tripp, P.; Behringer, D.; Hou, Y.-T.; Chuang, H.-Y.; Iredell, M.; et al. The NCEP Climate Forecast System Version 2. *J. Clim.* **2014**, *27*, 2185–2208. [CrossRef]
46. Laloyaux, P.; de Boisséson, E.; Dahlgren, P. CERA-20C: An Earth system approach to climate reanalysis. *ECMWF Newsl.* **2016**, *150*, 25–30. [CrossRef]
47. Mitchell, T.P.; Wallace, J.M. The annual cycle in equatorial convection and sea surface temperature. *J. Clim.* **1992**, *5*, 1140–1156. [CrossRef]

48. Moore, D.; Hisard, P.; McCreary, J.; Merle, J.; O'Brien, J.; Picaut, J.; Verstraete, J.M.; Wunsch, C. Equatorial adjustment in the eastern Atlantic. *Geophys. Res. Lett.* **1978**, *5*, 637–640. [CrossRef]
49. Brandt, P.; Caniaux, G.; Bourles, B.; Lazar, A.; Dengler, M.; Funk, A.; Hormann, V.; Giordani, H.; Marin, F. Equatorial upper-ocean dynamics and their interaction with the West African monsoon. *Atmos. Sci. Lett.* **2011**, *12*, 24–30. [CrossRef]
50. Rodríguez-Fonseca, B.; Mohino, E.; Mechoso, C.R.; Caminade, C.; Biasutti, M.; Gaetani, M.; García-Serrano, J.; Vizy, E.K.; Cook, K.; Xue, Y.; et al. Variability and Predictability of West African Droughts: A Review on the Role of Sea Surface Temperature Anomalies. *J. Clim.* **2015**, *28*, 4034–4060. [CrossRef]
51. Okumura, Y.; Xie, S.P. Interaction of the Atlantic Equatorial Cold Tongue and the African Monsoon. *J. Clim.* **2004**, *17*, 3589–3602. [CrossRef]
52. Meynadier, R.; De Coëtlogon, G.; Leduc-Leballeur, M.; Eymard, L.; Janicot, S. Seasonal influence of the sea surface temperature on the low atmospheric circulation and precipitation in the eastern equatorial Atlantic. *Clim. Dyn.* **2016**, *47*, 1127–1142. [CrossRef]
53. Diakhaté, M.; Lazar, A.; De Coëtlogon, G.; Gaye, A.T. Do SST gradients drive the monthly climatological surface wind convergence over the tropical Atlantic? *Int. J. Clim.* **2018**, *38*, e955–e965. [CrossRef]
54. Crespo, L.R.; Keenlyside, N.; Koseki, S. The role of sea surface temperature in the atmospheric seasonal cycle of the equatorial Atlantic. *Clim. Dyn.* **2019**, *52*, 5927. [CrossRef]
55. Druyan, L.M.; Fulakeza, M. The impact of the Atlantic cold tongue on West African monsoon onset in regional model simulations for 1998–2002. *Int. J. Clim.* **2015**, *35*, 275–287. [CrossRef]
56. Saravanan, R.; Chang, P. Oceanic mixed layer feedback and tropical Atlantic variability. *Geophys. Res. Let* **1999**, *26*, 3629–3632. [CrossRef]
57. Lindzen, R.S.; Nigam, S. On the role of sea surface temperature gradients in forcing low-level winds and convergence in the tropics. *J. Atmos. Sci.* **1987**, *44*, 2418–2436. [CrossRef]
58. Rodwell, M.J.; Hoskins, B.J. Subtropical anticyclones and summer monsoons. *J. Clim.* **2001**, *14*, 3192–3211. [CrossRef]
59. Miyasaka, T.; Nakamura, H. Structure and mechanisms of the Southern Hemisphere summertime subtropical anticyclones. *J. Clim.* **2010**, *23*, 2115–2130. [CrossRef]
60. Ji, X.; Neelin, J.D.; Lee, S.K.; Mechoso, C.R. Interhemispheric teleconnections from tropical heat sources in intermediate and simple models. *J. Clim.* **2014**, *27*, 684–697. [CrossRef]
61. Seager, R.; Murtugudde, R.; Naik, N.; Clement, A.; Gordon, N.; Miller, J. Air–sea interaction and the seasonal cycle of the subtropical anticyclones. *J. Clim.* **2003**, *16*, 1948–2019. [CrossRef]
62. Lee, S.K.; Mechoso, C.R.; Wang, C.; Neelin, J.D. Interhemispheric influence of the northern summer monsoons on southern subtropical anticyclones. *J. Clim.* **2013**, *26*, 10193–10204. [CrossRef]
63. Keenlyside, N.S.; Latif, M. Understanding equatorial Atlantic interannual variability. *J. Clim.* **2007**, *20*, 131–142. [CrossRef]
64. Lübbecke, J.F.; Böning, W.C.; Keenlyside, N.S.; Xie, S.P. On the connection between Benguela and equatorial Atlantic Niños and the role of the South Atlantic anticyclone. *J. Geophys. Res.* **2010**, *115*, C09015. [CrossRef]
65. Ding, H.; Greatbatch, R.J.; Latif, M.; Park, W. The impact of sea surface temperature bias on equatorial Atlantic interannual variability in partially coupled model experiments. *Geophys. Res. Lett.* **2015**, *42*, 5540–5546. [CrossRef]
66. Dippe, T.; Greatbatch, R.J.; Ding, H. On the relationship between Atlantic Niño variability and ocean dynamics. *Clim. Dyn.* **2018**, *51*, 597–612. [CrossRef]
67. Toniazzo, T.; Koseki, S. A Methodology for Anomaly Coupling in Climate Simulation. *J. Adv. Model. Earth Syst.* **2018**, *10*, 2061–2079. [CrossRef]
68. Lutz, K.; Rathmann, J.; Jacobeit, J. Classification of warm and cold water events in the eastern tropical Atlantic Ocean. *Atmos. Sci. Lett.* **2013**, *14*, 102–106. [CrossRef]
69. Florenchie, P.; Lutjeharms, J.R.; Reason, C.J.C.; Masson, S.; Rouault, M. The source of Benguela Niños in the south Atlantic Ocean. *Geophys. Res. Lett.* **2003**, *30*. [CrossRef]
70. Oettli, P.; Morioka, Y.; Yamagata, T. A regional climate model discovered in the North Atlantic: Dakar Niño/Niña. *Sci. Rep.* **2016**, *6*, 18782. [CrossRef] [PubMed]
71. Carton, J.A.; Huang, B. Warm events in the Tropical Atlantic. *J. Phys. Oceanogr.* **1994**, *24*, 888–903. [CrossRef]
72. Bjerknes, J. Atmospheric teleconnections from the equatorial Pacific. *Mon. Weather Rev.* **1969**, *97*, 163–172. [CrossRef]

73. Jouanno, J.; Hernandez, O.; Sanchez-Gomez, E. Equatorial Atlantic interannual variability and its relation to dynamic and thermodynamic processes. *Earth Sys. Dyn.* **2017**, *8*, 1061–1069. [CrossRef]
74. Deppenmeier, A.L.; Haarsma, R.J.; Hazeleger, W. The Bjerknes feedback in the tropical Atlantic in CMIP5 models. *Clim. Dyn.* **2016**, *47*, 2691–2707. [CrossRef]
75. Giordani, H.; Caniaux, G. Diagnosing vertical motion in the Equatorial Atlantic. *Ocean. Dyn.* **2001**, *61*, 1995–2018. [CrossRef]
76. Lübbecke, J.F.; McPhaden, M.J. Symmetry of the Atlantic Niño mode. *Geophys. Res. Lett.* **2017**, *44*, 965–973. [CrossRef]
77. Larkin, N.K.; Harrison, D.E. ENSO warm (El Niño) and cold (La Niña) event life cycles: Ocean surface anomaly patterns, their symmetries, asymmetries, and implications. *J. Clim.* **2002**, *15*, 1118–1140. [CrossRef]
78. Takahashi, K.; Dewitte, B. Strong and moderate nonlinear El Niño regimes. *Clim. Dyn.* **2016**, *46*, 1627–1645. [CrossRef]
79. Nnamchi, H.C.; Li, J.; Kucharski, F.; Kang, I.S.; Keenlyside, N.S.; Chang, P.; Farneti, R. Thermodynamic controls of the Atlantic Niño. *Nat. Commun.* **2015**, *6*, 8895. [CrossRef] [PubMed]
80. Richter, I.; Behara, S.K.; Masumoto, Y.; Taguchi, B.; Sasaki, H.; Yamagata, T. Multiple causes of interannual sea surface temperature variability in the equatorial Atlantic Ocean. *Nat. Geosci.* **2012**, *16*, NGEO1660. [CrossRef]
81. Brandt, P.; Funk, A.; Hormann, V.; Dengler, M.; Greatbatch, R.J.; Toole, J.M. Interannual atmospheric variability forced by the deep equatorial Atlantic Ocean. *Nature* **2011**, *473*, 497–500. [CrossRef] [PubMed]
82. Foltz, G.R.; McPhaden, M.J. Abrupt equatorial wave-induced cooling of the Atlantic cold tongue in 2009. *Geophys. Res. Lett.* **2010**, *37*. [CrossRef]
83. Burmeister, K.; Brandt, P.; Lübbecke, J.F. Revisiting the cause of the Eastern Equatorial Atlantic cold event in 2009. *J. Geophys. Res. Oceans* **2016**, *121*, 4777–4789. [CrossRef]
84. Martín-Rey, M.; Lazar, A. Is the coreal spring tropical Atlantic variability a precursor of the Equatorial Mode? *Clim. Dyn.* **2019**, *53*, 2339–2353. [CrossRef]
85. Lübbecke, J.F.; Burls, N.J.; Reason, C.J.; McPhaden, M.J. Variability in the South Atlantic anticyclone and the Atlantic Niño mode. *J. Clim.* **2014**, *27*, 8135–8150. [CrossRef]
86. Patricola, C.M.; Chang, P.; Saravanan, R. Degree of simulated suppression of Atlantic tropical cyclones modulated by flavour of El Niño. *Nat. Geo.* **2016**, *9*, 155. [CrossRef]
87. Lima, D.; Soares, P.M.M.; Semedo, A.; Cardoso, R.M. A Global View of Coastal Low-Level Wind Jets using an Ensemble of Reanalysis. *J. Clim.* **2018**, *31*, 1525–1546. [CrossRef]
88. Lima, D.C.; Soares, P.M.; Semedo, A.; Cardoso, R.M.; Cabos, W.; Sein, D.V. A Climatological Analysis of the Benguela Coastal Low-Level Jet. *J. Geophys. Res. Atmos.* **2019**, *124*, 3960–3978. [CrossRef]
89. Graham, N.E.; Barnett, T.P. Sea surface temperature, surface wind divergence, and convection over tropical oceans. *Science* **1987**, *238*, 657–659. [CrossRef]
90. Waliser, D.E.; Gautier, C. A satellite-derived climatology of the ITCZ. *J. Clim.* **1993**, *6*, 2162–2174. [CrossRef]
91. Koseki, S.; Bhatt, B.C. Unique relationship between tropical rainfall and SST to the north of the Mozambique Channel in boreal winter. *Int. J. Clim.* **2018**, *38*, e378–e387. [CrossRef]
92. Xie, S.P.; Philander, S.G.H. A coupled ocean-atmosphere model of relevance to the ITCZ in the eastern Pacific. *Tellus A* **1994**, *46*, 340–350. [CrossRef]
93. Amaya, D.J.; DeFlorio, M.J.; Miller, A.J.; Xie, S.P. WES feedback and the Atlantic Meridional Mode: Observations and CMIP5 comparisons. *Clim. Dyn.* **2017**, *49*, 1665–1679. [CrossRef]
94. Imbol Koungue, R.A.; Illig, S.; Rouault, M. Role of interannual Kelvin wave propagations in the equatorial Atlantic on the Angola–Benguela Current system. *J. Geophys. Res. Oceans* **2017**, *22*, 4685–4703. [CrossRef]
95. Rouault, M.; Florenchie, P.; Fauchereau, N.; Reason, C.J. South East tropical Atlantic warm events and southern African rainfall. *Geophys. Res. Lett.* **2003**, *30*, 5. [CrossRef]
96. Richter, I.; Behera, S.K.; Masumoto, Y.; Taguchi, B.; Komori, N.; Yamagata, T. On the triggering of Benguela Niños: Remote equatorial versus local influences. *Geophys. Res. Lett.* **2010**, *37*, L20604. [CrossRef]
97. Junker, T.; Schmidt, M.; Mohrholz, V. The relation of wind stress curl and meridional transport in the Benguela upwelling system. *J. Mar. Syst.* **2015**, *143*, 1–6. [CrossRef]
98. Sennel, W.; Junker, T.; Schmidt, M.; Mohrholz, V. Response of the Benguela upwelling systems to spatial variations in the wind stress. *Cont. Shelf Res.* **2012**, *45*, 65–77.

99. Junker, T. Response of the Benguela Upwelling System to Changes in the Wind Forcing. Ph.D. Thesis, University of Rostock, Rostock, Germany, 2014.
100. Xu, Z.; Chang, P.; Richter, I.; Kim, W.; Tang, G. Diagnosing southeast tropical Atlantic SST and circulation biases in the CMIP5 ensemble. *Clim. Dyn.* **2014**, *43*, 3123–3145. [CrossRef]
101. Florenchie, P.; Reason, C.J.C.; Lutjeharms, J.R.E.; Rouault, M.; Roy, C.; Masson, S. Evolution of interannual warm and cold events in the southeast Atlantic Ocean. *J. Clim.* **2004**, *17*, 2318–2334. [CrossRef]
102. Rouault, M.; Illig, S.; Bartholomae, C.; Reason, C.J.C.; Bentamy, A. Propagation and origin of warm anomalies in the Angola–Benguela upwelling system in 2001. *J. Mar. Syst.* **2007**, *68*, 4735–5488. [CrossRef]
103. Tokinaga, H.; Xie, S.P. Weakening of the equatorial Atlantic cold tongue over the past six decades. *Nat. Geos.* **2011**, *4*, 222. [CrossRef]
104. Mohino, E.; Rodríguez-Fonseca, B.; Mechoso, C.R.; Losada, T.; Polo, I. Relationships among Intermodel Spread and Biases in Tropical Atlantic Sea Surface Temperatures. *J. Clim.* **2019**. [CrossRef]
105. Martín-Rey, M.; Polo, I.; Rodríguez-Fonseca, B.; Losada, T.; Lazar, A. Is there evidence of changes in tropical Atlantic variability modes under AMO phases in the observational record? *J. Clim.* **2018**, *31*, 515–536. [CrossRef]
106. Losada, T.; Rodríguez-Fonseca, B. Tropical atmospheric response to decadal changes in the Atlantic Equatorial Mode. *Clim. Dyn.* **2016**, *47*, 1211–1224. [CrossRef]
107. Cabos, W.; Garcia, F.A.; Ortizbevia, M.J. Generation of equatorial Atlantic warm and cold events in a coupled general circulation model simulation. *Tellus* **2002**, *54*, 426–438.
108. Alvarez-Garcia, F.; Cabos, W.; Ortiz-Bevia, M. An Assessment of Differences in ENSO Mechanisms in a Coupled GCM Simulation. *J. Clim.* **2006**, *19*, 69–87. [CrossRef]
109. Ham, Y.G.; Kug, J.S.; Park, J.Y. Two distinct roles of Atlantic SSTs in ENSO variability: North tropical Atlantic SST and Atlantic Niño. *Geophys. Res. Lett.* **2013**, *40*, 4012–4017. [CrossRef]
110. Martín-Rey, M.; Rodríguez-Fonseca, B.; Polo, I.; Kucharski, F. On the Atlantic–Pacific Niños connection: A multidecadal modulated mode. *Clim. Dyn.* **2014**, *43*, 3163–3178. [CrossRef]
111. Park, J.-H.; Li, T. Interdecadal modulation of El Niño–tropical North Atlantic teleconnection by the Atlantic multi-decadal oscillation. *Clim Dyn.* **2019**, *52*, 5345–5360. [CrossRef]
112. Mohino, E.; Losada, T. Impacts of the Atlantic Equatorial Mode in a warmer climate. *Clim. Dyn.* **2015**, *45*, 2255–2271. [CrossRef]
113. Breugem, W.P.; Hazeleger, W.; Haarsma, R.J. Mechanism of northern tropical Atlantic variability and response to CO_2 doubling. *J. Clim.* **2007**, *20*, 2691–2705. [CrossRef]
114. Kucharski, F. Tropical Pacific response to 20th century Atlantic warming. *Geophys. Res. Lett.* **2011**, *38*, L03702. [CrossRef]
115. Choi, J.Y.; Ham, Y.G.; McGregor, S. Atlantic-Pacific SST Gradient Change Responsible for the Weakening of North Tropical Atlantic-ENSO Relationship due to Global Warming. *Geophys. Res. Lett.* **2019**. [CrossRef]
116. Ham, Y.G.; Kug, J.S.; Yang, W.H.; Cai, W. Future changes in Extreme El Nino events modulated by North Tropical Atlantic variability. *Geophys. Res. Lett.* **2018**, *45*, 6646–6653. [CrossRef]
117. Vizy, E.K.; Cook, K.H.; Sun, X. Decadal change of the south Atlantic ocean Angola–Benguela frontal zone since 1980. *Clim. Dyn.* **2018**, *51*, 3251. [CrossRef]
118. Taylor, K.E.; Stouffer, R.J.; Meehl, G.A. An overview of CMIP5 and the experiment design. *BAMS* **2012**, *93*, 485–498. [CrossRef]
119. Zuidema, P. Challenges and prospects for reducing coupled climate model SST biases in the eastern tropical Atlantic and Pacific oceans: The US CLIVAR Eastern Tropical Oceans synthesis working group. *BAMS* **2016**. [CrossRef]
120. Mechoso, C.R.; Robertson, A.W.; Barth, N.; Davey, M.K.; Delecluse, P.; Gent, P.R.; Ineson, S.; Kirtman, B.; Latif, M.; Le Treut, H.; et al. The seasonal cycle over the tropical Pacific in general circulation models. *Mon. Weather. Rev.* **1995**, *123*, 2825–2838. [CrossRef]
121. Richter, I. Climate model biases in the eastern tropical oceans: Causes, impacts and ways forward. *Interdiscip. Rev. Clim. Chang.* **2015**, *6*, 345–358. [CrossRef]
122. Hulme, M.; Doherty, R.; Ngara, T.; New, M.; Lister, D. African climate change: 1900-2100. *Clim. Res.* **2001**, *17*, 145–168. [CrossRef]
123. Huang, B.; Hu, Z.Z.; Jha, B. Evolution of model systematic errors in the tropical Atlantic basin from coupled climate hindcasts. *Clim. Dyn.* **2007**, *28*, 661–682. [CrossRef]

124. Bellucci, A.; Gualdi, S.; Navarra, A. The double-ITCZ syndrome in coupled general circulation models: The role of large-scale vertical circulation regimes. *J. Clim.* **2010**, *23*, 1127–1145. [CrossRef]
125. Li, G.; Xie, S.P. Tropical biases in CMIP5 multimodel ensemble: The excessive equatorial Pacific cold tongue and double ITCZ problems. *J. Clim.* **2014**, *27*, 1765–1780. [CrossRef]
126. Jiang, J.H.; Su, H.; Zhai, C.; Perun, V.S.; Del Genio, A.; Nazarenko, L.S. Evaluation of cloud and water vapor simulations in CMIP5 climate models using NASA "A-Train" satellite observations. *J. Geophys. Res. Atmos.* **2012**, *117*. [CrossRef]
127. Li, G.; Xie, S.P. Origins of tropical-wide SST biases in CMIP multi-model ensembles. *Geophys. Res. Lett.* **2012**, *39*, L22703. [CrossRef]
128. Harlaß, J.; Latif, M.; Park, W. Alleviating tropical Atlantic sector biases in the Kiel climate model by enhancing horizontal and vertical resolution: Climatology and interannual variability. *Clim. Dyn.* **2018**, *50*, 2605–2635. [CrossRef]
129. De la Vara, A.; Cabos, W.; Sein, D.; Sidorenko, D.; Koldunov, N.; Koseki, S.; Soares, P.M.M.; Danilov, S. On the impact of atmospheric vs oceanic resolutions on the representation of the sea surface temperature in the South Eastern Tropical Atlantic. *Clim. Dyn*. under review.
130. Small, R.J.; Curchitser, E.; Hedstrom, K.; Kauffman, B.; Large, W.G. The Benguela upwelling system: Quantifying the sensitivity to resolution and coastal wind representation in a global climate model. *J. Clim.* **2015**, *28*, 9409–9432. [CrossRef]
131. Wacongne, S.; Piton, B. The near-surface circulation in the northeastern corner of the South Atlantic Ocean. Deep Sea Research Part, A. *Oceanogr. Res. Pap.* **1992**, *39*, 1273–1298.
132. Lass, H.; Schmidt, M.; Mohrholz, V.; Nausch, G. Hydrographic and current measurements in the area of the Angola–Benguela front. *J. Phys. Oceanogr.* **2000**, *30*, 2589–2609. [CrossRef]
133. Exarchou, E.; Prodhomme, C.; Brodeau, L.; Guemas, V.; Doblas-Reyes, F. Origin of the warm eastern tropical Atlantic SST bias in a climate model. *Clim. Dyn.* **2018**, *51*, 1819–1840. [CrossRef]
134. Giese, B.S.; Carton, J.A. The Seasonal Cycle in Coupled Ocean-Atmosphere Model. *J. Clim.* **1994**, *7*, 1208–1217. [CrossRef]
135. Wahl, S.; Latif, M.; Park, W.; Keenlyside, N. On the tropical Atlantic SST warm bias in the Kiel climate model. *Clim. Dyn.* **2011**, *36*, 891–906. [CrossRef]
136. Hourdin, F.; Găinuşă-Bogdan, A.; Braconnot, P.; Dufresne, J.-L.; Traore, A.-K.; Rio, C. Air moisture control on ocean surface temperature, hidden key to the warm bias enigma. *Geophys. Res. Lett.* **2015**, *42*, 10885–10893. [CrossRef]
137. Voldoire, A.; Exarchou, E.; Sanchez-Gomez, E.; Demissie, T.; Deppenmeier, A.L.; Frauen, C.; Goubanova, K.; Hazeleger, W.; Keenlyside, N.; Koseki, S.; et al. Role of wind stress in driving SST biases in the Tropical Atlantic. *Clim. Dyn.* **2019**, 1–24. [CrossRef]
138. Shi, Y.; Huang, W.; Wang, B.; Yang, Z.; He, X.; Qiu, T. Origin of warm SST bias over the Atlantic cold tongue in the coupled climate model FGOALS-g2. *Atmosphere* **2018**, *9*, 275. [CrossRef]
139. Toniazzo, T.; Woolnough, S. Development of warm SST errors in the southern tropical Atlantic decadal hindcasts. *Clim. Dyn.* **2014**, *43*, 2889–2913. [CrossRef]
140. Zermeño-Diaz, D.M.; Zhang, C. Possible root causes of surface westerly biases over the equatorial Atlantic in global climate models. *J. Clim.* **2013**, *26*, 8154–8168. [CrossRef]
141. Richter, I.; Wittenberg, A.T.; Masumoto, Y. Tropical Atlantic biases and their relation to surface wind stress and terrestrial precipitation. *Clim. Dyn.* **2012**, *38*, 985–1001. [CrossRef]
142. Breugem, W.P.P.; Chang, C.J.; Jang, J. Mignot, and W. Hazeleger. Barrier layers and tropical Atlantic SST biases in coupled GCMs. *Tellus* **2008**, *60*, 885–897. [CrossRef]
143. Mechoso, C.R.; Losada, T.; Koseki, S.; Mohino, E.; Keenlyside, N.; Castaño, A.; Myers, T.; Rodríguez-Fonseca, B.; Toniazzo, T. Can reducing the incoming energy flux over the Southern Ocean in a CGCM improve its simulation of tropical climate? *Geophys. Res. Lett.* **2016**, *43*, 11057–11106. [CrossRef]
144. Danabasoglu, G.; Yeager, S.G.; Bailey, D.; Behrens, E.; Bentsen, M.; Bi, D. North Atlantic simulations in coordinated ocean-ice reference experiments phase II (CORE-II). Part I: Mean states. *Ocean. Model.* **2014**, *73*, 76–107. [CrossRef]
145. Hwang, Y.T.; Frierson, D.M. Link between the double-Intertropical Convergence Zone problem and cloud biases over the Southern Ocean. *Proc. Natl. Acad. Sci. USA* **2013**, *110*, 4935–4940. [CrossRef]

146. Seo, H.; Jochum, M.; Murtugudde, R.; Miller, A.J. Effect of ocean mesoscale variability on the mean state of tropical Atlantic climate. *Geophys. Res. Lett.* **2006**, *33*, L090606. [CrossRef]
147. Harlaß, J.; Latif, M.; Park, W. Improving climate model simulation of tropical Atlantic sea surface temperature: The importance of enhanced vertical atmosphere model resolution. *Geophys. Res. Lett.* **2015**, *42*, 2401–2408. [CrossRef]
148. Doi, T.; Vecchi, G.A.; Rosati, A.J.; Delworth, T.L. Biases in the Atlantic ITCZ in seasonal-interannual variations for a coarse-And a high-resolution coupled climate model. *J. Clim.* **2012**, *25*, 5494–5511. [CrossRef]
149. Bonino, G.; Masina, S.; Iovino, D.; Storto, A.; Tsujino, H. Eastern Boundary Upwelling Systems response to different atmospheric forcing in a global eddy-permitting ocean model. *J. Mar. Sys.* **2019**, *197*, 103178. [CrossRef]
150. Sein, D.V.; Koldunov, N.V.; Danilov, S.; Sidorenko, D.; Wekerle, C.; Cabos, W. The relative influence of atmospheric and oceanic model resolution on the circulation of the North Atlantic Ocean in a coupled climate model. *J. Adv. Model. Earth* **2018**, *10*, 2026–2041. [CrossRef]
151. Richter, I.; Xie, S.P.; Behera, S.K.; Doi, T.; Masumoto, Y. Equatorial Atlantic variability and its relation to mean state biases in CMIP5. *Clim. Dyn.* **2014**, *42*, 171–188. [CrossRef]
152. Wang, C.; Zhang, L.; Lee, S.K.; Wu, L.; Mechoso, C.R. A global perspective on CMIP5 climate model biases. *Nat. Clim. Change* **2014**, *4*, 201–205. [CrossRef]